RSM ANALYSIS OF BEAD GEOMETRY OF SAW PROCESS AND MODELLING USING ANN.

Submitted in the partial fulfillment of the requirement

For the award of Degree of

MASTER OF ENGINEERING

IN

PRODUCTION ENGINEERING

Submitted by:

Jagtar Singh

14/PRO/06
(University Roll No.12651)

Under the Guidance

of:

Dr. D.S Nagesh

Asst. Professor

Department of Mechanical Engineering
Delhi College of Engineering, Delhi University

July -2009

CERTIFICATE

DELHI COLLEGE OF ENGINEERING
UNIVERSITY OF DELHI
(Govt. of National Capital Territory of Delhi)
BAWANA ROAD, DELHI - 110042

Date:-_____

This is certified that the work contained in this dissertation entitled **"RSM ANALYSIS OF BEAD GEOMETRY OF SAW PROCESS AND MODELLING USING ANN."** by **Mr. JAGTAR SINGH** is the requirement of the partial fulfillment for the award of Degree of **Master of Engineering (M.E.)** in **Production Engineering** at **Delhi College of Engineering**. This work was completed under my supervision and guidance. He has completed his work with utmost sincerity and diligence. The work embodied in this major project has not been submitted for the award of any other degree to the best of my knowledge.

Dr. D. S. Nagesh
Asst. Professor
Department of Mechanical Engineering
Delhi College of Engineering, Delhi

ACKNOWLEDGEMENT

I am thankful to the Almighty because without his blessings this work was not possible. It is a great pleasure to have the opportunity to extent my heartfelt gratitude to everybody who helped me throughout the course of this project.

It is distinct pleasure to express my deep sense of gratitude and indebtedness to my guide **Dr. D.S. Nagesh**, Mechanical Engineering Department for his invaluable guidance, patient reviews and continuous encouragement during all stages of thesis. His help in the form of valuable information and research papers at proper time has brought life in this thesis. I feel lucky to get an opportunity to work with him. I am thankful to the kindness and generosity shown by him towards me, as it helped me morally complete the project before actually starting it. I would like to thank Mr. Vinay (Welding Lab In Charge), Mr. Pradeep (Metallurgical Lab In Charge), Mr. Rahul Mool (Metrology Lab In Charge), and Mr. Manjeet singh for their cooperation. Without their support it would have been almost impossible to complete my thesis work in time.

I would also like to extend my sincere thanks to all faculty members of the Mechanical Engineering Department for the moral support and encouragement they had given to me during the project.

Last, but not the least, I would like to thank my family members for their help, encouragement and prayers through all these months. I dedicate my work to them.

(JAGTAR SINGH)
Roll No. 14/prod/06
University Roll No. 12651

ABSTRACT

One of the main welding processes used in the industries for the purpose of fabrication of huge sized structures is Submerged Arc Welding process. The key features of this process are high deposition rates and long weld runs.

The important process variables in submerged arc welding are: welding current, arc voltage, welding speed, nozzle to plate distance etc. The effects of these process variables are determined through their effects on weld bead geometry.

Design of experiment using response surface methodology was used to conduct experiment and to develop relationship for predicting weld bead geometry, which enables to quantify the direct and interaction effects. The response factors, namely penetration, bead width, and bead height, as affected by arc voltage, current welding speed and nozzle-to-plate distance have been investigated and analysed. The models developed have been checked for their adequacy and significance by using the F-test and the t-test, respectively. Main and interaction effects of the process variables on weld bead geometry are presented in graphical form. The developed models can be used for prediction of important weld bead dimensions and control of the weld bead quality by selecting appropriate process parameter values.

Use of artificial neural network to model submerged arc welding process is explored in present work. Back–propagation neural networks are used to associate the welding process variables with the features of bead geometry. These networks have yielded satisfactory generalization. A neural network could be effectively implemented for estimating the weld bead geometry.

INDEX

LIST OF TABLES

LIST OF FIGURES

LIST OF SYMBOLS

Symbol	Represents	Units
p	Weld penetration	mm
w	Weld width	mm
h	Weld bead height	mm
V	Arc voltage	volts
A	Arc current	amp
S	Welding speed	mm/min
N	Nozzle-to-plate distance	mm

Abreviations

SAW	Submerged arc welding
RSM	Response Surface Welding
ANN	Artificial Neural Network
NPD	Nozzle-to-plate distance
HAZ	Heat affected zone
WM	Weld metal
BM	Base metal

Chapter - 1

INTRODUCTION

INTRODUCTION

1.1Introduction

Submerged Arc Welding (SAW) is a versatile metal joining process in industry. It is a multi-variable, multi-objective metal fabrication process, characterized by the use of granulated fusible flux which covers the molten weld pool during operation. This arrangement facilitates slower cooling rate prevents, atmospheric contamination into weld pool and improves both mechanical properties and metallurgical characteristics of the weld bead as well as Heat Affected Zone (HAZ).

To have better control and knowledge of SAW process, it is essential to establish the relationship between process parameters and weld bead geometry to predict and control weld bead quality. The Design Of Experiments using Responsive Surface Methodology (RSM) technique may be used for establishing quantitative relationships between welding process parameter and weld bead geometry.

1.2 Motivation and Objectives

The motivation was provided by the desire to explore the potential of SAW process. For exploiting the potential of the process to great extent possible, basic understanding of the process is mandatory.

The main objective of this project was to study the effects of SAW process parameters such as arc voltage, current, travelling speed and nozzle-to-plate distance on weld bead geometry, and to develop mathematical model for evaluating the effects of welding process parameters on the weld bead geometry .Further prediction of bead geometry using Artificial Neural Network (ANN).

1.3 Statement of problem.

"RSM for analysis of bead geometry of SAW and modelling using ANN."

This research work describes the development of mathematical models based on practical observations, made during SAW of mild steel by bead-on-plate technique to estimate accurately the weld bead dimensions as affected by welding process variables and predicting the bead geometry using ANN.

1.4 Plan of investigation.

For accomplishment of the desired aim, the research work was planned to be carried out in the following steps:

- Identifying the important process control variables.
- Selection of the useful limits of the welding parameters,viz. voltage (V), current (A), travelling speed (S), and nozzle to plate distance (N).
- Developing the design matrix.
- Conducting the experiment as per design matrix.
- Recording the responses viz. penetration (P), bead width (w) & reinforcement height (H).
- Development of mathematical models.
- Calculating the co-efficient of polynomial.
- Checking adequacy of the models developed.
- Prediction of results using feed forward back propogation neural network.
- Analysis of results and conclusion.

Chapter - 2

LITERATURE REVIEW

2.0 LITERATURE REVIEW

Welding is a fabrication process that joins materials, usually metals or thermoplastics, by causing coalescence. This is often done by melting the workpieces and adding a filler material to form a pool of molten material that cools to become a strong joint, the process is carried out with pressure sometimes used in conjunction with heat, or only with heat, to produce the weld. Many different energy sources can be used for welding, including a gas flame, an electric arc, a laser, an electron beam, friction, and ultrasound. While often an industrial process, welding can be done in many different environments, including open air, under water and in outer space. Engineers became conscious of the quality of the welded joints since about 1950s. Weld bead geometric parameters have a large influence on the quality of the product is now well understood and accepted. The studies on the effects of various welding process parameters on the formation of bead, depth of penetration and bead geometry have attracted the attention of many researchers to carry out further investigations. Recent developments in the evolution of artificial neural networks have been found to be useful in solving many engineering problems. In different fields of engineering, back-propagation neural network has proved to be one of the best algorithms for predictive type of work. Design of experiment (DOE) combined with Response surface methodology (RSM) is a powerful statistical tool to determine and represent the cause and effect relationship between true mean responses and input control variables influencing the responses as a two or three dimensional hyper surface.

The present literature review has been carried out in the areas concerning the effects of various welding parameters on bead geometry, application of artificial neural network in welding in optimization of process parameters and application of RSM to develop mathematical relationship between the welding process parameters and the output variables of the welded joint.

2.1 Effects of welding process parameters on bead geometric characteristics.

The bead geometry of the weld bead is the major factors influencing the structural adequacy of the weld, such as its strength. Some of the weld bead characteristics of significance are bead width, bead height, penetration, etc. The properties of the welded joints are affected by a large number of these weld bead parameter .The correlation between welding process parameters and bead geometry characteristics can provide useful information about the quality of the welds. Researchers, to describe the weld bead geometry, have identified various welding process parameters affecting the resulting bead geometry. The following literature review makes an attempt to provide an insight in to the above-mentioned area.

R.S. Chandel et al.[3] presented theoretical predictions of the effect of current, electrode polarity, electrode diameter and electrode extension on the melting rate, bead height, bead width and weld penetration, in submerged-arc welding. They studied that the melting rate of SAW can be increased by four methods: (i) using higher current; (ii) using straight polarity; (iii) using a smaller diameter electrode; and (iv) using a longer electrode extension. The percentage difference in melting rate, bead height, bead width, and bead

penetration is affected by the current level and polarity. When a smaller diameter electrode is used, the increase in the current level does not make much difference to the percentage change in bead height, bead width, and weld penetration.

Investigation on pulsed tugsten arc welding parameters was done by **G. Lothongkum et al. [7].** In their study TIG pulse welding parameters of AISI 316L stainless steel plate of 3 mm thickness at the welding positions of 6±12 h were investigated. The studied parameters were welding speed, pulse/base currents, and pulse frequency. Pure argon and argon with nitrogen contents of 1±4 vol.% were used as shielding gas. Preliminary welding results at the 6 h welding position showed that the appropriate parameters were: base current of 61 A, pulse frequency of 5 Hz, and 65% on time. With these constant parameters the effects of welding speeds of 2±8 mm/s and nitrogen contents of 0±4 vol.% in argon shielding gas on pulse currents were examined to attain acceptable weld bead profile corresponding to DIN 8563 class BS with complete penetration. The results showed that the lowest pulse currents were observed at the 9 h welding position. Increasing nitrogen content in argon gas decreases the pulse currents. At the welding positions of 6 and 12 h, the maximum welding speed is limited to 6 mm/s, and with a welding speed of 7 mm/s the formation of slag inclusion at the top of weld metal was observed. The depth/width ratios (D/W) are between 0.34 and 0.40. Increasing welding speed decreases in the weld width and increases in the D/W ratio. Radiography showed acceptable weld beads free of porosity.

D. Kim et.al. [11] proposed a method for determining the near-optimal settings of welding process parameters using a Controlled Random Search

(CRS) wherein the near-optimal settings of the welding process parameters are determined through experiments. The method suggested in this study is used to determine the welding process parameters by which the desired weld bead geometry is formed in Gas Metal Arc (GMA) welding. In this method, the output variables (front bead height, back bead width, and penetration) are determined by the input variables (wire feed rate, welding voltage, and welding speed). The number of levels for each input variable and the total search points were determined to be 10 and 1000, respectively.

Erdal Karadeniz et al. [18] in their study, the effects of various welding parameters on welding penetration in Erdemir 6842 steel having 2.5 mm thickness welded by robotic gas metal arc welding were investigated. The welding current, arc voltage and welding speed were chosen as variable parameters. The depths of penetration were measured for each specimen after the welding operations and the effects of these parameters on penetration were researched. The welding currents were chosen as 95, 105, 115 A, arc voltages were chosen as 22, 24, and 26 V and the welding speeds were chosen as 40, 60 and 80 cm/min for all experiments. As a result of this study, it was found that increasing welding current increased the depth of penetration. In addition, arc voltage is another parameter in incrimination of penetration. However, its effect is not as much as current's. The highest penetration was observed in 60 cm/min welding current.

Serdar Karaoglu, Abdullah Secgin[23] studied that selection of process parameters has great influence on the quality of a welded connection. Mathematical modelling can be utilized in the optimization and control procedure of parameters. Rather than the well-known effects of main process

parameters, this study focuses on the sensitivity analysis of parameters and fine tuning requirements of the parameters for optimum weld bead geometry. Changeable process parameters such as welding current, welding voltage and welding speed are used as design variables. The objective function is formed using width, height and penetration of the weld bead. Experimental part of the study is based on three level factorial design of three process parameters. In order to investigate the effects of input (process) parameters on output parameters, which determine the weld bead geometry, a mathematical model is constructed by using multiple curvilinear regression analysis. After carrying out a sensitivity analysis using developed empirical equations, relative effects of input parameters on output parameters are obtained. Effects of all three design parameters on the bead width and bead height show that even small changes in these parameters play an important role in the quality of welding operation. The results also reveal that the penetration is almost non-sensitive to the variations in voltage and speed.

The influence of the (SAW) process parameters (welding current and welding speed) on the microstructure, hardness, and toughness of HSLA steel weld joints has been investigated by **Keshav Prasad,D.K. Dwivedi[26].** Attempts have also been made to analyze the results on the basis of the heat input. The SAW process was used for the welding of 16 mm thick HSLA steel plates. The weld joints were prepared using comparatively high heat input (3.0 to 6.3 KJ/mm) by varying welding current (500–700 A) and welding speed (200–300 mm/min). Results showed that the increase in heat input coarsens the grain structure both in the weld metal and Heat Affected Zone (HAZ). The hardness has been found to vary from the weld centre line to base metal and

peak hardness was found in the HAZ. The hardness of the weld metal was largely uniform. The hardness reduced with the increase in welding current and reduction in welding speed (increasing heat input) while the toughness showed mixed trend. The increase in welding current from 500 A to 600 A at a given welding speed (200 mm/min or 300 mm/min) increased toughness and further increase in welding current up to 700 A lowered the toughness. Scanning electron microscopy of the fractured surfaces of impact test specimen was carried out to study the fracture modes. Electron Probe Micro Analysis (EPMA) was carried out to investigate the variation in wt.% of different elements in the weld metal and HAZ.

From the discussion on the above-mentioned literature it is observed that in different welding processes the weld bead parameters such as penetration, bead width, reinforcement height etc are largely influenced by various welding parameters such as arc current, voltage, travelling speed, In pulsed tungsten arc welding it is found that by increasing welding speed will increase the pulse current and increasing nitrogen contents in argon gas decreases the pulse currents, and then the solubility of nitrogen in the weld decreases. Increasing welding speed more than 6 mm/s results in the formation of slag inclusion at the top of welds. In SAW the melting rate can be increased by four methods: (i) using higher current; (ii) using straight polarity; (iii) using a smaller diameter electrode; and (iv) using a longer electrode extension. In robotic GMA welding applied to Erdemir 6842 steel sheets having 2.5 mm thickness the depth of penetration increases linearly with increasing welding current between 95 and 115 A and the average penetration rise was measured as 0.0225 mm for each 1 A current increment. It can be concluded from these revelations that bead

geometry parameters such as penetration, bead width etc are influenced by various parameters under different welding conditions using different welding processes.

2.2 Application of artificial neural network in welding in optimization of process parameters

Artificial Neural Networks (ANN) has remarkable ability to derive meaning from complicated or imprecise data. They can be used to detect trends that are too complex to be noticed by either humans or other computer techniques. A trained neural network can act like an expert in the category of information it has been given to analyze. It can then be used to provide projections given new situations of interest. Their ability to learn by example makes them very flexible and powerful. They are very well suited for real time systems because of their fast response and computational times, which are due to their parallel architecture. ANN are being used by researchers in various engineering applications The following literature survey has been made to study the application of ANN in welding and other engineering problems.

George E. Cook et al. [1] evaluated artificial neural networks for monitoring and control of the Variable Polarity Plasma Arc Welding process. Three areas of welding application were investigated: weld process modeling, weld process control, and weld bead profile analysis for quality control.

D.S. Nagesh, G.L. Datta[8] in their work used artificial neural networks to model the shielded metal-arc welding process. Back-propagation neural networks are used to associate the welding process variables with the

features of the bead geometry and penetration. These networks have achieved good agreement with the training data and have yielded satisfactory generalization. A neural network could be effectively implemented for estimating the weld bead and penetration geometric parameters. The results of these experiments show a small error percentage difference between the estimated and experimental values.

I.S. Kim et al. [9] developed an intelligent algorithm to understand relationships between process parameters and bead height, and to predict process parameters on bead height through a neural network and multiple regression methods for robotic multi-pass welding process. In this work a series of robotic arc welding, additional multi-pass butt welds were carried out in order to verify the performance of the neural network estimator and multiple regression methods as well as to select the most suitable model. The results indicated that neural network model proved to be better than the empirical models having linear and curvilinear equations.

Ill-Soo Kim et al. **[10]** in their research, made an attempt to develop a neural network model to predict the weld bead width as a function of key process parameters in robotic GMA welding. The neural network model is developed using two different training algorithms; the error back-propagation algorithm and the Levenberg–Marquardt approximation algorithm. The accuracy of the neural network models developed in this study has been tested by comparing the simulated data obtained from the neural network model with that obtained from the actual robotic welding experiments. The result shows that the Levenberg–Marquardt approximation algorithm is the preferred method, as

this algorithm reduces the root of the mean sum of squared (RMS) error to a significantly small value.

Veerendra Singh et.al. [17] carried out a detailed statistical analysis on plant data to study relationship of raw material and furnace performance. Feed forward back propogation neural network with three different learning algorithim were tried to improve the prediction accuracy.

This study of **Abdulkadir C`evik et al [24]** presents, neural network (NN) for the prediction of ultimate capacity of arc spot welding. The proposed NN model is based on experimental results. The ultimate capacity of arc spot welding is modelled in terms of weld strength, average welding thickness and diameter. The results of the proposed NN model are later compared with results of existing codes and are found to more accurate. Parametric studies are also carried out to analyze the effect of each variable.

The development of a back propagation neural network model for the prediction of weld bead geometry in pulsed gas metal arc welding process has been studied by **K. Manikya Kanti, P. Srinivasa Rao[25]**. The model is based on experimental data. The thickness of the plate, pulse frequency, wire feed rate, wire feed rate/travel speed ratio, and peak current have been considered as the input parameters and the bead penetration depth and the convexity index of the bead as output parameters to develop the model. The developed model is then compared with experimental results and it is found that the results obtained from neural network model are accurate in predicting the weld bead geometry.

In the literature survey, it is found that ANN has been emerging as one of the powerful predictive tools for application in engineering applications. It has also been used in some of the welding processes, which are in most of the cases very complex systems involving large number of parameters leaving scope for further work. In the present work artificial neural network approach is being used as a predicting tool for submerged arc welding process using experimental data.

2.3 Application of Response Surface Methodology (RSM) for modeling and optimization of process

Response surface methodology (RSM) is a technique to determine and represent the cause and effect relationship between true mean response and input control variables influencing the response as a two or three dimensional hyper surface. The steps involved in RSM technique are as follows:

- Designing of a set of experiment for adequate and reliable measurement of the true mean response of interest.
- Determination of mathematical model with best fits
- Finding the optimum set of experimental factors that produces maximum or minimum value of response
- Representing the direct and interactive effects of process variables on the best parameters through two dimensional and three dimensional graphs.

The accuracy and effectiveness of an experiment depends on careful planning and execution of the experimental procedure. A number of researchers have applied RSM to manufacturing environment. Some very

useful work carried out in the areas concerning has been reported in the present literature review.

Bappa Acherjee et. al.[30] made a study to investigate the effect of process parameters ,namely, laser power ,welding speed, size of laser beam and clamp pressure, on the lap-shear strength and weld-seam width for laser transmission welding of acrylic, using a diode laser system. RSM was employed to devlop mathematical relationships between the welding process parameters and the output variables of the weld joint to determine the welding input parameters that lead to the desired weld quality. In addition, using response surface plots, the interaction effects of process parameters on the responses were analyzed and discussed.

An attempt was also made to relate green compression strength to mould hardness by **M B Parappagoudar et. al. [20]** using Design of experiments (DOE) with response surface methodology. A Pareto optimal front of solutions was developed for strength and permeability, using a multiobjective optimization tool called non-dominated sorting genetic algorithm (NSGA). The Pareto optimal front contains a number of optimal solutions. One optimal solution differs from another on account of the fact that different sets of weightages are given to the objective functions. Thus, the user has to select one set of optimal solutions

out of different available sets.

The main problem faced in the manufacturing of pipes by the SAW process, was the selection of the optimum combination of input variables for achieving the required qualities of the weld. This problem was solved by **V. Gunaraj** et**. al**. **[5]** by developing mathematical models through effective and strategic

planning and the execution of experiments by RSM.They used a four-factor five level central composite rotatable design matrix with full replication for planning, conduction, execution and development of mathematical model.

P B Bacchewar et. al. [21] studied the effect of process parameters, namely build orientation, laser power, layer thickness, beam speed, and hatch spacing, on surface roughness. Central rotatable composite design (CCD) of experiments was used to plan the experiments. Analysis of variance (ANOVA) was used to study the significance of process variables on surface roughness. In the case of upward-facing surfaces, build orientation and layer thickness was found to be significant parameters. In downward facing surfaces, other than build orientation and layer thickness, laser power had also been found to be significant. Empirical models were developed for estimating the surface roughness of the parts. A trust-region-based optimization method had been employed to obtain a set of process parameters for obtaining the best surface finish. A confirmation experiment had been carried out at an optimum set of parameters and predicted results were found to be in good agreement with experimental findings.

P Thangavel et. al.[15] evaluated the impact of factors such as cutting speed, feed rate, and depth of cut on flank wear of a high speed steel (HSS) cutting tool during the turning process of a mild steel component. A mathematical model was developed relating flank wear and the main factors such as cutting speed V, feed rate F, and depth of cut T. Response surface methodology (RSM) was used to

develop the mathematical model and the model was checked for adequacy by regression analysis. Main and interaction effects of the control factors on flank

wear were presented in graphical form, which helps in selecting quickly the process parameters to achieve the desired quality of machining surface by way of controlling the wear of the cutting tool.

A mathematical model was presented by **Godfrey C. Onwubolu. Et. al.[16]** for correlating the interactions of some drilling control parameters such as speed, feed rate and drill diameter and their effects on some responses such as axial force and torque acting on the cutting tool during drilling by means of response surface methodology. For this exercise, a three-level full factorial design was chosen for experimentation using a PC-based computer numerically controlled drilling machine built in-house. The significance of the mathematical model developed was ascertained using Microsoft Excel® regression analysis module. The results obtained shows that the mathematical model is useful not only for predicting optimum process parameters for achieving the desired quality but for process optimization. Using the optimal combination of these parameters is useful in minimizing the axial force and torque of drilling operations; by extension, other drilling parameters such as cutting pressure, material removal rate, and power could be optimized since they depend on the combination of drilling parameters which affect the axial force and torque.

The application of response surface methodology was highlighted by **V. Balasubramanian et. al.[31]** to predict and optimize the percentage of dilution of iron-based hardfaced surface produced by the PTA (plasma transferred arc welding) process. The experiments were conducted based on five-factor five-level central composite rotatable design with full replication technique and a mathematical model was developed using response surface

methodology. Furthermore, the response surface methodology was also used to optimize the process parameters that yielded the lowest percentage of dilution.

A.M.K. Hafiz et. al.[22] developed an effective method to predict surface roughness for high speed end milling of AISI H13 tool steel using PCBN inserts.The response surface methodology (RSM) has been utilized for the postulation of a second order quadratic model in terms of cutting speed, axial depth of cut and feed. Sufficient numbers of experiments were run based on the Box-Wilson central composite design (CCD) concept of RSM in order to generate roughness data. The ANOVA technique has been used to verify the adequacy of the model at 95% confidence interval. From the model it was found that feed plays the most dominating role on surface finish followed by the cutting speed. However, axial depth of cut does not have significant effect on roughness value. The roughness tends to decrease with decreasing feed and increasing cutting speed.

2.4 Conclusion

The literature review has brought about an understanding of the effects of welding process variables on weld bead geometry, use of RSM technique to determine and represent the cause and effect relationship between true mean response and input control variables influencing the response as a two or three dimensional hyper surface and use of artificial neural networks in the prediction of weld bead geometry in various welding process.

However ,an integrated approach of studying the effects of various welding process variables on bead geometric descriptors using response surface methodology technique and predicting the weld bead geometry using artificial

neural networks is hardly found in literature. Thus on this literature review the objective for the present work have been outlined.

Objective of the present investigation includes the following:

- Identifying the important process control variables.
- Selection of the useful limits of the welding parameters.
- Developing the design matrix and conducting the experiment as per design matrix.
- Recording the responses .
- Development of mathematical models.
- Calculating the co-efficient of polynomial.
- Checking adequacy of the models developed.
- Prediction of results using feed forward back propogation neural network.
- Analysis of results and conclusion.

Chapter - 3

THEORY AND EXPERIMENTATION

3.1 Submerged Arc Welding (SAW)

3.1.1 Introduction

Submerged Arc Welding (SAW) is a high quality welding process with a very high deposition rate. It is commonly used to join thick sections in the flat position. It requires a continuously fed consumable solid or tubular (metal cored) electrode. The wire is fed continuously to the arc by a feed unit of motor-driven rollers. The flux is fed from a hopper fixed to the welding head and a tube from hopper spreads the flux in a continuous manner in front of the arc.

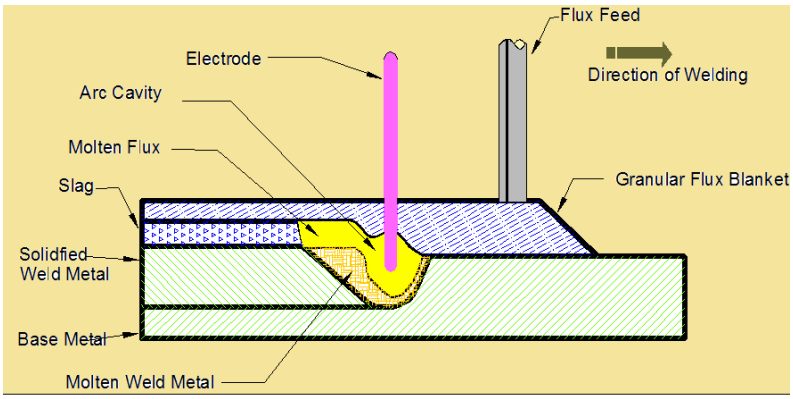

Fig.3.1 Sectional view of SAW process

The molten weld and the arc zone are protected from atmospheric contamination by being “submerged” under a blanket of granular fusible flux. When molten, the flux becomes conductive, and provides a current path between the electrode and the work. Sectional view of SAW process is shown in fig 3.1 SAW is usually operated either as fully mechanized or automatically processed, however, semi-automatic (hand-held) During SAW process, operator cannot observe the weld pool and not directly interfere with the welding process. As the automation in the SAW process increases, direct effect of the operator decreases and the precise setting of parameters

become much more important than manual welding processes.. Currents ranging from 200 to 1500 A are commonly used. Currents of up to 5000 A have been used (multiple arcs).). DC or AC power can be utilized, and combinations of DC and AC are common on multiple electrode systems.

Constant Voltage welding power supplies are most commonly used, however Constant Current systems in combination with a voltage sensing wire-feeder are available.

The potential advantages of mechanized welding, several attempts were made to mechanize the arc welding process developing a continuous coated electrode as an extension of manual metal arc welding electrode was ruled out for the following reason:

- Since the Coating is non-conducting, arranging electrical contact with the electrode is not practicable.
- The coating is likely to peel off when the electrode is coiled.
- The coating is also likely to get crushed when fed through the feed rolls.

Since the introduction of SAW in 1935 there has been a continuing interest in the increase of productivity without deterioration in weld quality. In submerged arc welding the weld deposit quality is determined by following parameters

- Welding current
- Arc voltage
- Grade of wire used
- Travel speed
- Electrode stick-out
- Type of flux

- Size of electrode
- To get optimum result one must know the effect of above parameters on bead geometry, how to select them and control then properly.

3.1.2 SAW Equipment

The basic SAW equipment is shown in fig 3.2 .For a semi automatic system ,it consists of a welding power source, a wire feeder and control system, an automatic welding head, a flux hopper and a travel mechanism which usually consist of a travelling carriage and the rails.

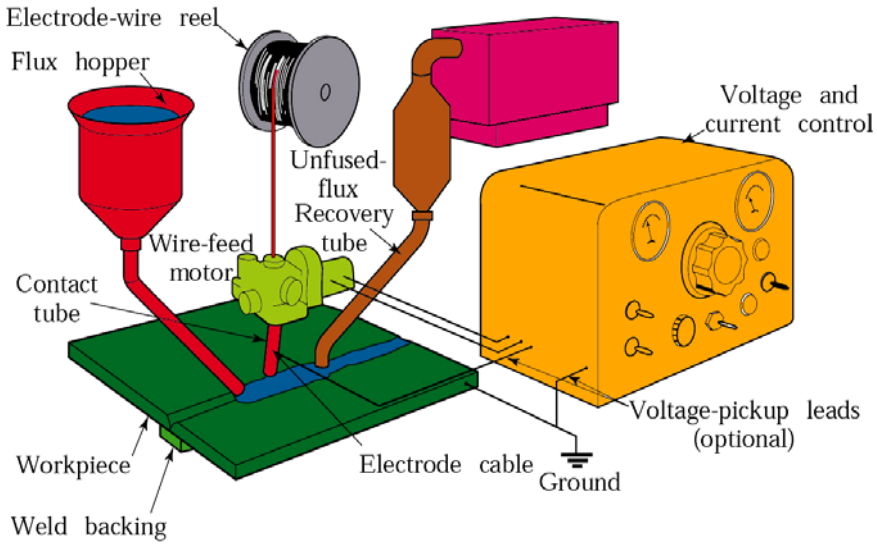

Fig:3.2 SAW machine in operation, courtesy http://materialteknologi.hig.no

3.1.3 Process

The submerged arc welding process creates an arc column between the wire electrode and the work piece .The electrode stick-out, the arc column and the weld pool are all submerged in a blanket of finely divided granulated powder that contains appropriate deoxidisers, cleanser and other desired fluxing

in gradients. The flux is fed from the hopper which is an integral part of the welding head. The flux flows through a tube and spread along joint edges ahead of the electrode in the form of a heap of desired height which is controlled by the tube to plate distance. The flux layer is of sufficient depth to avoid spatter and smoke and it protects the weld pool from the ill effects of atmosphere gases. This results in a smooth weld bead. The flux in contact with the hot metal melts and provides a protective layer of slag on top of the weld bead. The unmelted flux acts as an insulator and is reclaimed for reuse. The slag that forms on the weld bead normally peels off on its own or alternatively can be detached with the help of a chipping hammer.

3.1.3.1 Process features

SAW involves formation of an arc between a continuously-fed bare wire electrode and the work piece similar to MIG welding. The process uses a flux to generate protective gases and slag, and to add alloying elements to the weld pool. A shielding gas is not required. Prior to welding, a thin layer of flux powder is placed on the work piece surface. Remaining fused slag layers can be easily removed after welding. As the arc is completely covered by the flux layer, heat loss is extremely low. This produces a thermal efficiency as high as 60% (compared with 25% for manual metal arc). There is no visible arc light, welding is spatter-free and there is no need for fume extraction.

3.1.3.2 Operating characteristics:

SAW is usually operated as a fully-mechanized or automatic process, but it can be semi-automatic. Welding parameters: current, arc voltage and travel

speed all affect bead shape, depth of penetration and chemical composition of the deposited weld metal. Because the operator cannot see the weld pool, greater reliance must be placed on parameter settings.

3.1.3.3. Nomenclature of Weld Bead:

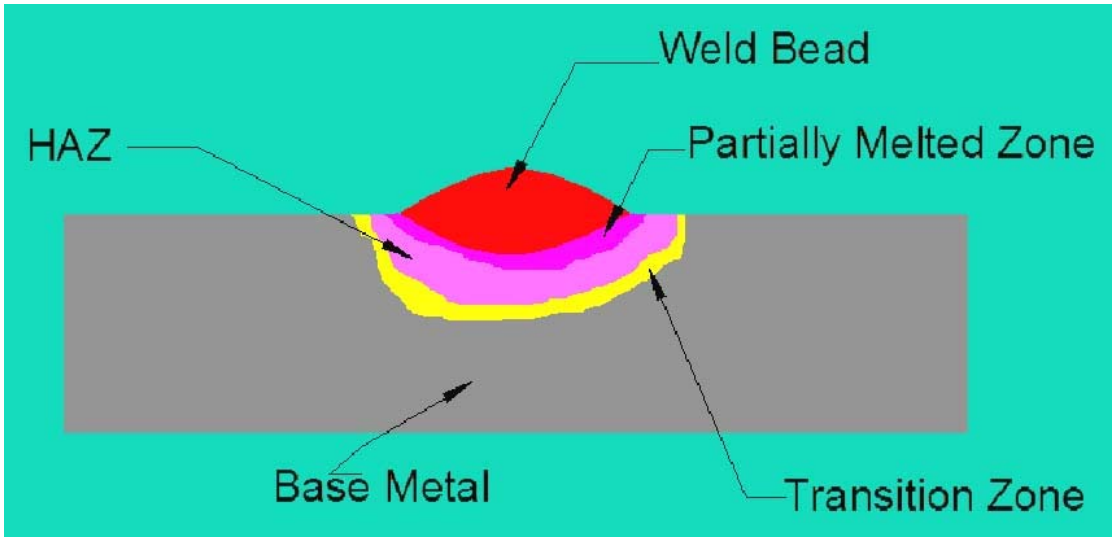

Fig :3.3 Nomenclature of Weld bead.

Nomenclature of weld bead is shown in fig.3.3 .In order to obtain high quality welds in automated welding processes, selection of optimum parameters should be performed according to engineering facts. Therefore, it is important to study stability of welding parameters to achieve high quality welding.

Weld Bead Geometry - The mechanical properties of the welded joints greatly depend on weld bead geometry, which in turn, is influenced by welding parameters like arc current, arc voltage, and arc travel speed. The bead geometry is specified by weld bead width, reinforcement height, reinforcement area, penetration height, penetration area and the contact angle of weld bead etc.

The Weld Bead Width is the maximum width of the weld metal deposited. It

increases with arc current, arc voltage; electrode weaving and decreases as arc travel speed increases.

Penetration Height or simply penetration is the distance from base plate top surface to the maximum extent of the weld nugget. Penetration determines the load carrying capacity of a welded structure.

Penetration Area is that covered by the fusion line below the base metal level. Penetration area affects the weld strength.

Reinforcement Height is the maximum distance between the base metal level and the top point of the deposited metal.

Reinforcement Area is one included between the contour line of the deposited metal above the base metal level.

3.1.4 Wire

SAW is normally operated with a single wire on either AC or DC current. Common variants are:

- twin wire
- triple wire
- single wire with hot wire addition
- metal powder addition

All contribute to improved productivity through a marked increase in weld metal deposition rates and/or travel speeds.

Other factors:

• Flux depth/width;

• Flux and electrode classification and type;

• Electrode wire diameter;

• Multiple electrode configurations.

3.1.5 SAW Fluxes [37].

Most metals in their molten condition become oxidized by the absorption of oxygen from the atmosphere .To make certain that amount of oxidation is kept a minimum, that any oxides formed are dissolved or floated off,and that welding is made as easy and free from difficulties as possible, fluxes are used.Fluxes,therefore are chemical compound used to prevent oxidation and other unwanted chemical reactions. They help to make the welding process easier and ensure the making of a good, sound weld.

Fluxes for Submerged arc welding usually consist of metallic oxides such as CaO,MgO and FeO and fluorides such as CaF2.The flux is specially formulated to be compatible with a given electrode wire type so that the combination of flux and wire yields desired mechanical properties. All fluxes react with the weld pool to produce the weld metal chemical composition and mechanical properties. Like the manual electrode coating the SAW Flux can incorporates alloying elements. So that in combination with an unalloyed wire it will yield suitably alloyed weld metal. The molten slag also provides favourable conditions for very high current densities which, together with the insulating properties with the flux, concentrate heat into a relatively small welding zone. This results in deeply penetrating arc, which makes narrower and shallower welding grooves practicable, thus reducing the amount of weld metal required to complete the joint. It also results in higher welding speeds. The properties of the flux enables submerged arc welds to be made over a wide range of welding currents voltage and speeds, each of which can be controlled independently of the other. Thus one can obtain welded joints of

desired shapes, chemistry and mechanical properties by using an appropriate welding procedure.

The SAW flux should be so formulated so it does not evolve appreciable amount of gases under intense heat of welding zone. It should be granular in form and should be capable of flowing freely through the flux feeding tubes, valves and nozzles of standard welding equipment. Its particle size should be controlled. The flux in its solid state is a non-conductor of electricity, but when in molten condition it becomes highly conducting medium. It is therefore necessary to initiate the arc by special means. Once the arc is stuck and the surrounding flux becomes molten, the welding current continues to flow across the arc, while the arc provides a conducting path of molten flux as it advances. The flux contains elements capable of assisting in the initial striking of arc and also of stabilizing it after initiation. It is common practice to refer to fluxes as 'active' if they add manganese and silicon to the weld, the amount of manganese and silicon added is influenced by the arc voltage and the welding current level.

3.1.5.1 Classification of SAW Fluxes:

SAW fluxes can be classified into two main groups:

- According to the method of manufacturing.
- According to the chemical nature.

3.1.5.1.1 According to the method of manufacturing:

SAW can be classified according to the methods by which the are manufactured. There are mainly two methods of manufacturing the flux.

3.1.5.1.1.1 Fused Fluxes. The constituents such as quartz, limestone and manganese dioxide (MnO_2) with small quantities of fluorspar and aluminium oxide (Al_2O_3) are melted in an electric arc furnace where the manganese dioxide (MnO_2) is reduced to MnO. When the melt attains the state of a glossy paste it can be cooled, crushed and then grounded, and suitable grain size obtained by sieving, the grains being about 0.2-1.6 mm diameter. This type of flux is homogeneous and was the first type of flux used.

3.1.5.1.1.2 Agglomerated Fluxes. These are more easily manufactured than the fused type, being made at a lower temperature. They are heterogeneous because they include compounds in powder form whose grains join together by the agglomeration process and make larger grains, each grain having the correct proportion of each component. The dry powder is fed into a rotating disc with the addition of water glass (a concentrated and viscous solution of sodium and potassium silicate) as a binding agent. The grains are then furnace- dried at about 700-800 °C and then sieved to give grain somewhat the same as for fused flux, 0.2-1.6 mm.

3.1.5.1.2 According to the chemical nature

The chemical nature of a welding flux can be expressed as the basicity or Basicity index.

$$B\ (\text{Basicity}) = \frac{Cao + MgO + CaF_2 + Na_20 + K_20 + 1/2(MnO + FeO)}{SiO2 + 1/_2(Al_2O_3 + TiO_2 + ZrO_2)}$$

The formula of basicity or Basicity index is based upon the ratio of basic oxide to acidic oxides.

Welding fluxes can thus be divided as shown in table 3.1.

Welding Flux	**Basicity**	**Melting Point (°C)**
Acidic	≦0.9	1100-1300
Neutral	= 0.9 – 1.2	1300-1500
Basic	=1.2 - 2.0	＞1500
High Basic	＞2.0	＞1500

Table 3.1 Classification of SAW fluxes

3.1.6 SAW Process Variables:

All the variables have a certain effect upon the bead geometry and rate of the deposit weld material. It is very essential to set several variables to correct range before starting SAW for achieving good quality welds. Following are the Process variables in SAW

- Welding current
- Arc voltage
- Travel speed
- Size of electrode
- Electrode stick out
- Heat input rate

3.1.6.1 Welding Current:

It controls the melting rate of the electrode and thereby the weld deposition rate. It also controls the depth of penetration. Too high a current causes excessive weld reinforcement, which is wasteful, and burn through in case of thinner plates or in badly fitted joints, which are not proper backing. Excessive current also produces too narrow bead and undercut, excessively low current gives an unstable arc and overlapping. SAW control panel is usually provided with an ammeter to monitor and control the welding current.

3.1.6.2. Arc Voltage

The arc voltage varies in direct proportion to the arc length. With the increase in arc length the arc voltage increases and thus more heat is available to melt the metal and the flux. However, increased arc length means more spread of the arc column; this leads to increase in weld width and volume of reinforcement while the depth of penetration decreases. The arc voltage varies with the welding current and wire diameter.

3.1.6.3 Travel Speed:

For a given combination of welding current and voltage, increase in welding speed results in lesser penetration, lesser weld reinforcement and lower heat input rate Excessively high travel speed, decreases fusion between the weld deposit and the parent metal, increases the tendencies for undercut , arc blow, porosity and irregular bead shape. As the speed decreases, penetration and reinforcement increases but too slow a speed result in poor penetration. Excessively high welding speed decreases the wetting action and increases

the probability of undercutting, arc blow, and weld porosity and uneven bead shapes. Excessively low speed also produces a convex hat shape beads that are subjected to cracking cause excessively melt through and produces a large weld puddle that flows around the arc resulting in rough bead, spatter and slag inclusions.

3.1.6.4 Size of Electrode

For a given welding current, a decrease of wire diameter results in increase in current density. This results in a weld with deeper penetration bue somewhat reduced width. The submerged arc welding process usually employs wires of 2 to 5 mm diameter, thus for deeper penetration at low currents a wire diameter 2 to 3 mm is best suited.

3.1.6.5 Electrode Stick out:

It is also termed as electrode extension. It refers to the length of electrode between end of contact tube and the arc, which is subjected to resistance heating at the high current densities used in the process. The longer the stick out, the increase in deposition rate is accompanied by a decrease in penetration. Hence longer stick-out is avoided when deep penetration is desired.

3.1.6.6. Heat Input Rate:

The heat input rate is directly proportional to the current and voltage and inversely proportional to the travel speed, as the formula is given by

$$HIR = \frac{V \times A}{S}$$

where HIR= heat input rate in j/mm

V = Arc voltage

A= welding current (amp)

S= Arc travel speed in mm/sec

For a given joint thickness, higher the heat input rate the lower is the cooling rate of the weld metal and heat affected zone of parent metal and vice versa. Heat input rate has an important bearing on the weld metal microstructure and the final microstructure of HAZ and thereby on the toughness.

3.1.7 Submerged Arc Welding Benefits:

- Extremely high deposition rates possible.
- Sound welds are readily made (with good process design and control).
- Deep weld penetration.
- High speed welding of thin sheet steels at over 100 in/min (2.5 m/min) is possible.
- Easily automated
- Minimal welding fume or arc light is emitted.
- Low operator skill required.

3.1.8 Limitations of SAW

- Limited to ferrous (steel or stainless steels) and some nickel based alloys.
- Normally limited to the 1F, 1G, and 2F positions.

- Normally limited to long straight seams or rotated pipes or vessels.
- Requires relatively troublesome flux handling systems.
- Flux and slag residue can present a health & safety issue.
- Requires inter-pass and post weld slag removal.

3.1.9 Applications:

SAW is ideally suited for longitudinal and circumferential butt and fillet welds. However, because of high fluidity of the weld pool, molten slag and loose flux layer, welding is generally carried out on butt joints in the flat position and fillet joints in both the flat and horizontal-vertical positions. For circumferential joints, the work piece is rotated under a fixed welding head with welding taking place in the flat position. Depending on material thickness, either single-pass, two-pass or multipass weld procedures can be carried out. There is virtually no restriction on the material thickness, provided a suitable joint preparation is adopted. Most commonly welded materials are carbon-manganese steels, low alloy steels and stainless steels, although the process is capable of welding some non-ferrous materials with judicious choice of electrode filler wire and flux combinations.

Major application in industry:

- Used in manufacturing of ship and heavy structural parts.
- Nowadays it is widely used in repairing of machine parts by depositing cladding and hard facing.
- Fabrication of pipes, penstocks, pressure vessels, boiler, railroad, structure of railway coaches and locomotive.
- Automotive, Aviation and nuclear industry.
- For welding mild steel, medium & high tensile low alloy

3.2 ARTIFICIAL NEURAL NETWORK (ANN)

3.2.1 Introduction

It is often called as "Neural Network" (NN), is a mathematical model or computational model based on biological neural networks. It consists of an interconnected group of artificial neurons and processes information using a connectionist approach to computation. In most cases an ANN is an adaptive system that changes its structure based on external or internal information that flows through the network during the learning phase. It is used to find patterns in data.

Neural networks are designed to incorporate key features of neurons in the brain and to process data in a manner analogous to the human brain. Much of the terminology used to describe and explain neural networks is borrowed from biology. Neural networks use a series of neurons in what is known as the hidden layer that apply nonlinear activation functions to approximate complex functions in the data.

We will now turn to the biological basis for the processing element that is the neuron. Neurons, or nerve cells, are the basic units of communication in nervous systems. Like processing elements, neurons do not act alone. They collectively sense environmental change, integrate sensory inputs, and then activate different body parts that carry out responses. These tasks involve different classes of neurons, called sensory neurons, interneurons, and motor neurons.

Sensory neurons are receptors that can detect specific stimuli, such as light energy, and relay them as signals to the brain and spinal cord. This is where

interneurons integrate these signals and then influence other neurons in turn. Interneurons in the brain and spinal cord are the "information processors" of the nervous system.

Motor neurons relay information away from the interneurons to muscle cells or gland cells, which carry out responses. The neurons which will be discussed here are of the interneuron type. It has been estimated that there are about 100 billion interneurons (henceforth called neurons) in the brain.

3.2.2 Basic Structure of Neuron

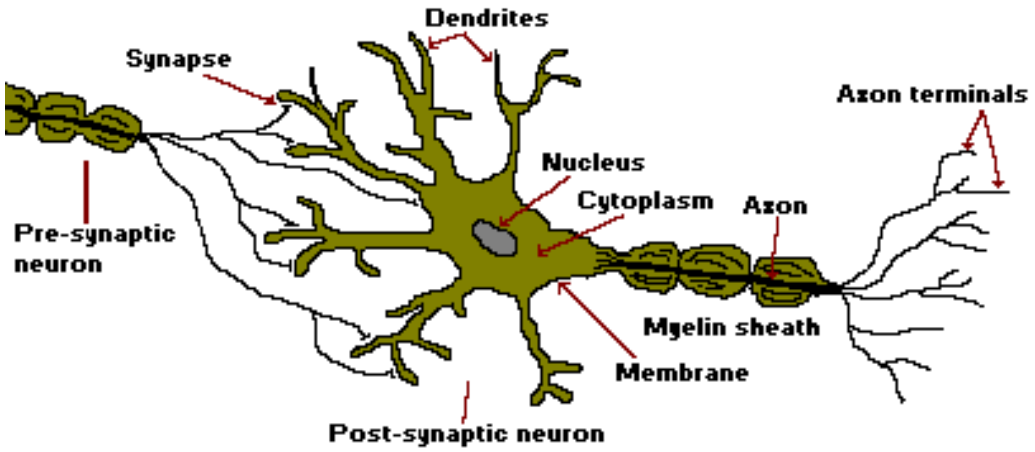

Fig 3.4: Basic structure of a neuron

A neuron, like any human cell, has a membrane that separates internal metabolic events from the environment and allows them to proceed in organized, controlled ways. It also has receptors that can alter the cell's activities by allowing molecules to go in and/or out of the cell. It also has a nucleus, which is contained within another membrane and holds the DNA, and other molecules that function in how, and which, instructions are read, modified, dispersed into the rest of the cell. The "rest of the cell" is known as

the cytoplasm, and is everything enclosed by the membrane, except for the nucleus.

A neuron contains many short slender extensions, called Dendrites, and a long cylindrical extension, called an Axon. Dendrites serve as the "input signals" for the neuron, receiving stimuli from other neurons. The number, length, branching, and synaptic activity of a neuron's dendrites depends upon its location and/or function and contributes to the vast information processing capacity of the brain.

The singular axon serves as the "output signal" of the neuron by which messages are sent to other cells This "output signal" is known as a nerve impulse. Neurons are not physically connected to each other. They communicate via the exchange of the neurotransmitters. Between an Axon terminal of one neuron, called the presynaptic neuron, and a Dendrite of another neuron, called the postsynaptic neuron, is a small gap known as a Synapse.

3.2.3 The Processing Element of ANN

A processing element is generally a simple device that receives a number of input signals that may or may not generate an output signal based upon those signals. For each input (xi) there is a relative weight(wi) associated with it such that the effective input to the processing element is the weighted total input(I).

$$I = \sum_{i=1}^{n} (w_i \cdot x_i)$$

The output(Y) is computed as a result of a transfer function (f) of the weighted input, or Y = f(I). Normally, the transfer function for a given processing element is fixed at the time that the network is constructed. So when one wants to change the output for a given input, the weights of the inputs are changed. This transfer function, also known as an input-output function, generally falls into one of three classes: Threshold, Linear, and sigmoidal

Threshold Units In threshold type processing elements; the weighted input is compared to an arbitrary threshold (T). This threshold value is often 0, which assumes that negatively valued inhibitory inputs are used. If the input is less than the threshold value, then the processing element does not fire and no output signal is generated.

Linear Units A network that computes real-valued functions needs processing elements whose transfer functions produce real-valued outputs. The simplest such type is the linear unit whose output signal equals its weighted sum input, thus giving a real-valued output, albeit linear in nature.

Sigmoidal Units the problem with linear type processing elements is that their transfer functions are not differentiable. Because of this fact, networks using linear type processing elements are difficult to train. To overcome the linear behaviour of networks using linear-threshold type transfer functions, smooth nonlinear transfer functions, which are continuous and differentiable everywhere, are often used. Of these, the sigmoidal type is most popular.

The output of a sigmoidal unit asymptotically goes to 1 as the weighted sum of its inputs approaches positive infinity and to 0 as the weighted sum of its inputs approaches negative infinity. This function is defined as: f (x) = 1/(1 + e(-x)), where x is the net input to the unit.

Fig 3.5 summarizes the three classes of processing elements. The horizontal axis for each type represents the net input showing a higher weighted sum as you go from left to right. The vertical axis represents the activity of the output going from lower to higher as it goes away from the horizontal axis.

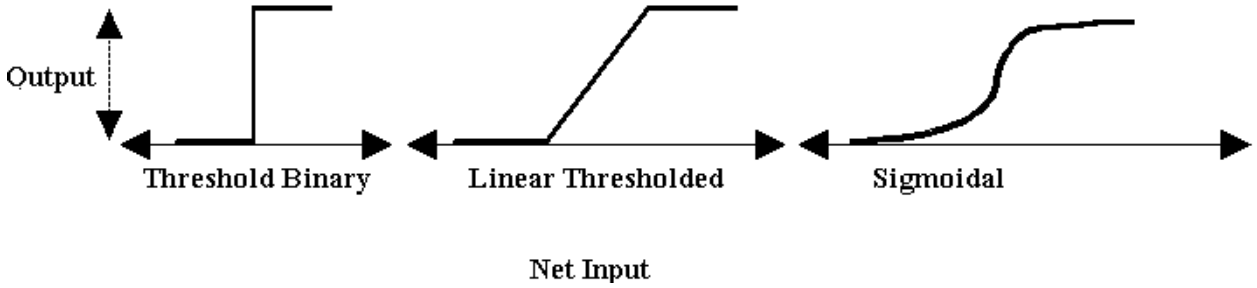

Fig 3.5: The three basic classes of transfer functions

3.2.4 Artificial Neural Networks Architectures

Artificial Neural networks are mathematical entities that are modeled after existing biological neurons found in the brain. All the mathematical models are based on the basic block known as artificial neuron. A simple neuron is shown in fig 3.6 This is a neuron with a single R-element input vector is shown below. Here the individual element inputs are multiplied by weights and the weighted values are fed to the summing junction. Their sum is simply Wp, the dot product of the (single row) matrix W and the vector p.

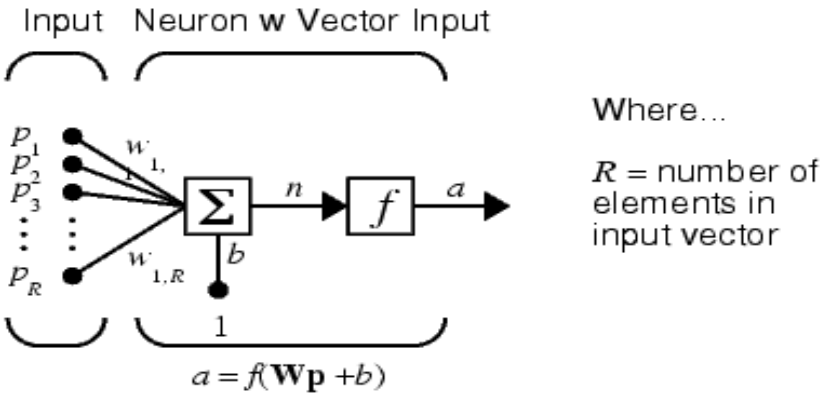

Fig 3.6. Simple neuron

The neuron has a bias b, which is summed with the weighted inputs to form the net input n. This sum, n, is the argument of the transfer function f.

Introducing vector notations, Fig 3.6 can be rewritten in a more compact representation as seen in Fig 3.7

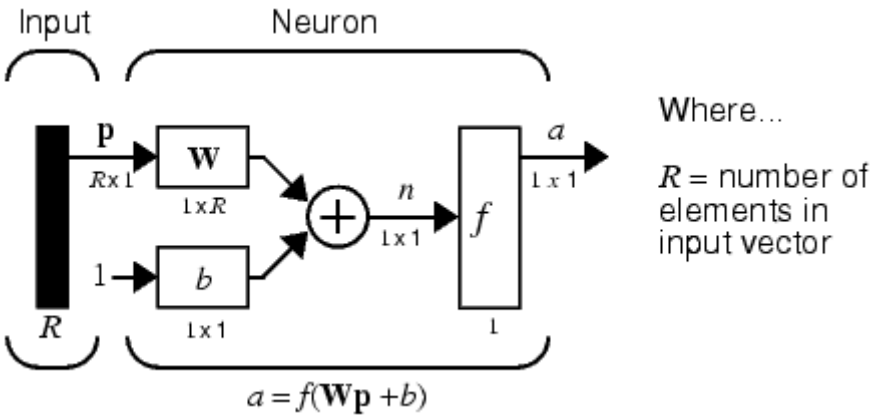

Fig. 3.7. Simple neuron in vector notation.

Here the input vector p is represented by the solid dark vertical bar at the left. The dimensions of p are shown below the symbol p in the figure as Rx1. Thus, p is a vector of R input elements. These inputs post multiply the single row, R column matrix W. As before, a constant 1 enters the neuron as an input and is multiplied by a scalar bias b. The net input to the transfer function f is n, the sum of the bias b and the product Wp. This sum is passed to the transfer function f to get the neuron's output a, which in this case is a scalar. Note that if we had more than one neuron, the network output would be a vector. A one-layer network with R input elements and S neurons is shown in Fig 3.9 In this network, each element of the input vector p is connected to each neuron input through the weight matrix W. The ith neuron has a summer that gathers its weighted inputs and bias to form its own scalar output n(i).

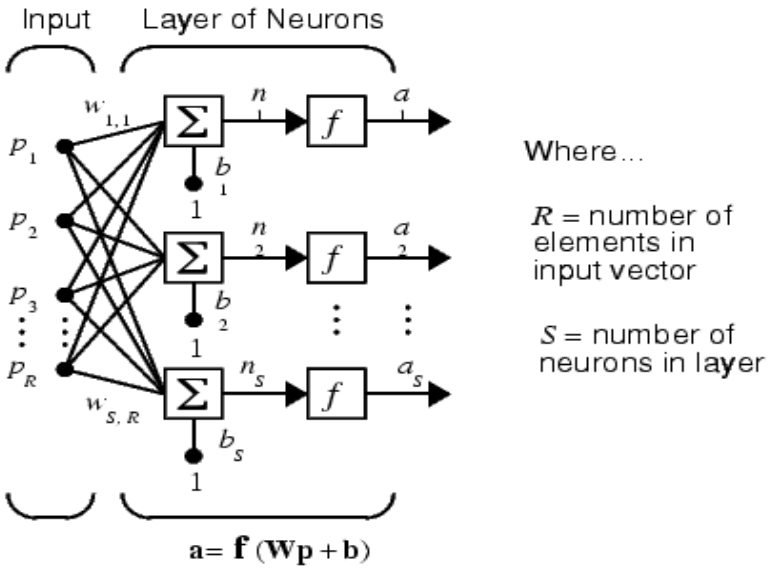

Fig. 3.8. One-layer network.

The various n (i) taken together form an S-element net input vector n. Finally, the neuron layer outputs form a column vector a.

Note that it is common for the number of inputs to a layer to be different from the number of neurons (i.e., R≠S). A layer is not constrained to have the number of its inputs equal to the number of its neurons.

You can create a single (composite) layer of neurons having different transfer functions simply by putting two of the networks shown earlier in parallel. Both networks would have the same inputs, and each network would create some of the outputs.

The input vector elements enter the network through the weight matrix W.

$$\mathbf{W} = \begin{bmatrix} w_{1,1} & w_{1,2} & \cdots & w_{1,R} \\ w_{2,1} & w_{2,2} & \cdots & w_{2,R} \\ & & & \\ w_{S,1} & w_{S,2} & \cdots & w_{S,R} \end{bmatrix}$$

The S neuron R input one-layer network also can be drawn in abbreviated notation.

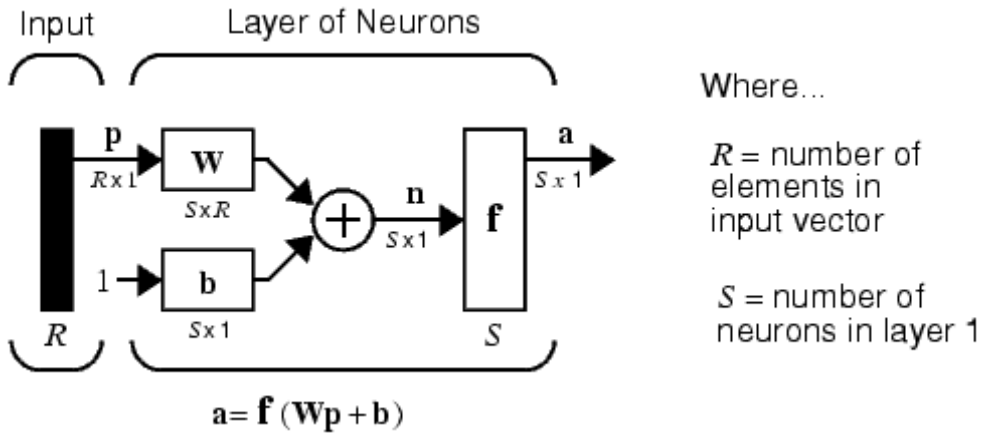

Fig.3.9. One-layer network in vector notation.

Here p is an R length input vector, W is an S x R matrix, and a and b are S length vectors. As defined previously, the neuron layer includes the weight matrix, the multiplication operations, the bias vector b, the summer, and the transfer function boxes.

A network can have several layers. Each layer has a weight matrix W, a bias vector b, and an output vector a. To distinguish between the weight matrices, output vectors, etc., for each of these layers in our figures, we append the number of the layer as a superscript to the variable of interest. You can see the use of this layer notation in the three-layer network shown below, and in the equations at the bottom of the Fig 3.10

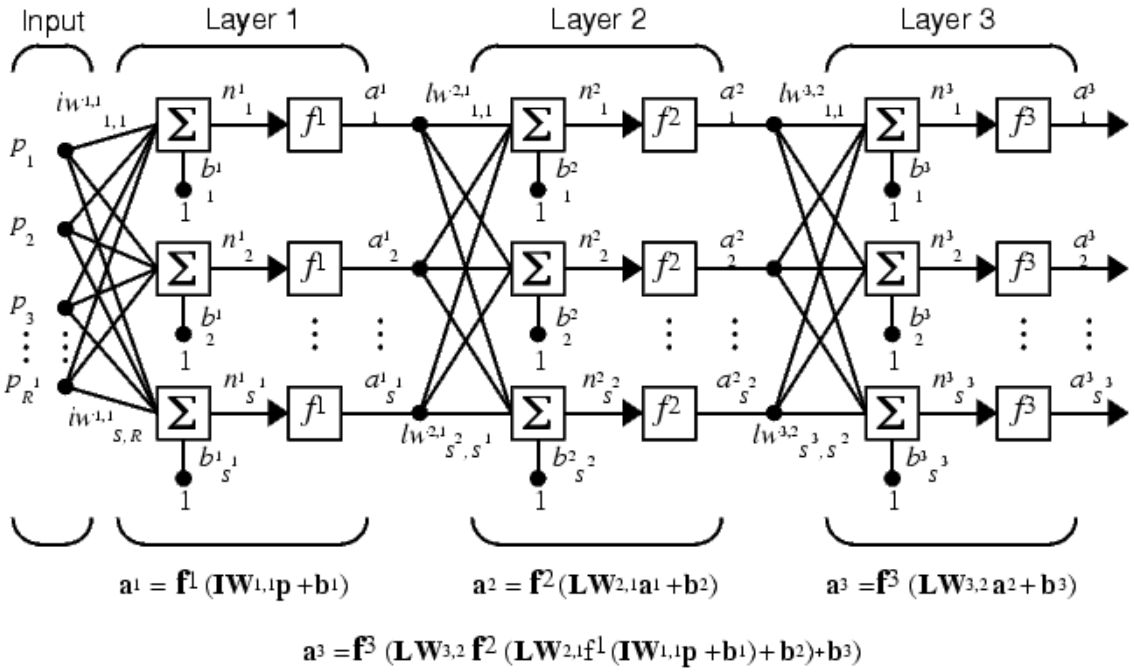

Fig 3.10. Multi-layer network.

The network shown above has R^1 inputs, S^1 neurons in the first layer, S^2 neurons in the second layer, etc. It is common for different layers to have different numbers of neurons. A constant input 1 is fed to the biases for each neuron. Note that the outputs of each intermediate layer are the inputs to the following layer. Thus layer 2 can be analyzed as a one-layer network with S^1 inputs, S^2 neurons, and an $S^2 \times S^1$ weight matrix W^2. The input to layer 2 is a^1; the output is a^2. Now that we have identified all the vectors and matrices of layer 2, we can treat it as a single-layer network on its own. This approach can be taken with any layer of the network.

The layers of a multilayer network play different roles. A layer that produces the network output is called an output layer. All other layers are called hidden layers. The three-layer network shown earlier has one output layer (layer 3) and two hidden layers (layer 1 and layer 2).

The same three-layer network discussed previously also can be drawn using our abbreviated notation.

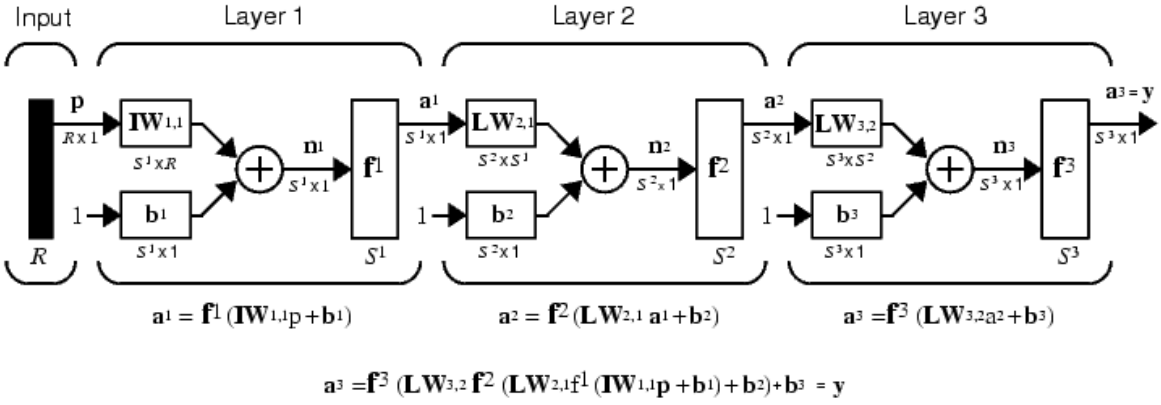

Fig.3.11. Multi-layer network in vector notation.

Multiple-layer networks are quite powerful. For instance, a network of two layers, where the first layer is sigmoid and the second layer is linear, can be trained to approximate any function (with a finite number of discontinuities) arbitrarily well. Here we assume that the output of the third layer, a^3, is the network output of interest, and we have labelled this output as y. We will use this notation to specify the output of multilayer networks.

The previous networks considered are Feed forward in the sense of the flow of information through the network.

3.3 RESPONSE SURFACE METHODOLOGY (RSM):

3.3.1 Introduction:

Response surface methodology (RSM) is a collection of statistical and mathematical techniques useful for developing, improving, and optimizing process. It also has important application in the design, development, and formulation of new products, as well as in the improvement of existing product designs. The most extensive application of RSM are in the industrial world, particularly in situations where several input variables potentially influence some performance measure or quality characteristic of the product or process. This performance measure or quality characteristic is called Response. It is typically measured on a continuous scale, although attribute responses, ranks and sensory responses are not unusual. Most of the real world application of RSM will involve more than one response. The input variables are sometimes called independent variables and they are subject to the control of the engineer or scientist, at least for the purpose of a test or an experiment.

3.3.2 Central Composite Designs (CCD)

A Box-Wilson Central Composite Design commonly called ‘a central composite design,' contains an imbedded factorial or fractional factorial design with centre points that is augmented with a group of `star points' that allow estimation of curvature. If the distance from the centre of the design space to a factorial point is ±1 unit for each factor, the distance from the centre of the design space to a star point is ±α with |α| > 1. The precise value of α

depends on certain properties desired for the design and on the number of factors involved.

Similarly, the number of centre point runs the design is to contain also depends on certain properties required for the design.

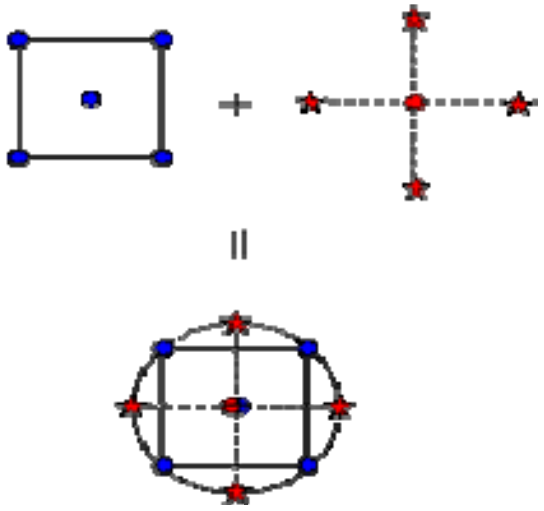

Fig 3.12:- Generation of a Central Composite Design for two factors

A central composite design always contains twice as many star points as there are factors in the design. The star points represent new extreme values (low and high) for each factor in the design. Table3.2 summarizes the properties of the three varieties of central composite designs. Fig 3.12 illustrates the relationships among these varieties.

Central Composite Design Type	**Terminology**	**Comments**
Circumscribed	CCC	CCC designs are the original form of the central composite design. The star points are at some distance α from the center based on the properties desired for the design and the

		number of factors in the design. The star points establish new extremes for the low and high settings for all factors. Figure 5 illustrates a CCC design. These designs have circular, spherical, or hyper spherical symmetry and require 5 levels for each factor. Augmenting an existing factorial or resolution V fractional factorial design with star points can produce this design.
Inscribed	CCI	For those situations in which the limits specified for factor settings are truly limits, the CCI design uses the factor settings as the star points and creates a factorial or fractional factorial design within those limits (in other words, a CCI design is a scaled down CCC design with each factor level of the CCC design divided by α to generate the CCI design). This design also requires 5 levels of each factor.
Face Centred	CCF	In this design the star points are at the center of each face of the factorial space, so $\alpha = \pm 1$. This variety requires 3 levels of each factor. Augmenting an existing factorial or resolution V design with appropriate star points can also produce this design.

TABLE:3.2 Central Composite Designs

3.3.2.1 Comparison of the 3 central composite designs:

The diagrams in fig:-3.13 illustrate the three types of central composite designs for two factors. Note that the CCC explores the largest process space and the CCI explores the smallest process space. Both the CCC and CCI are rotatable designs, but the CCF is not.

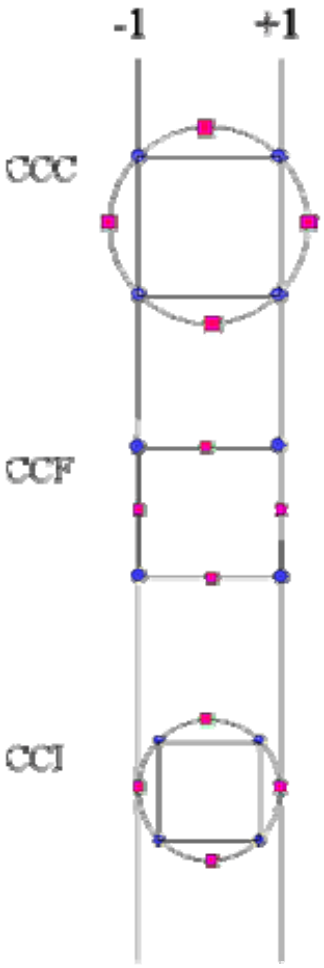

Fig 3.13 Comparison of the Three Types of Central Composite Designs

3.3.3 Plan of investigation.

For accomplishment of the desired aim, the research work was planned to be carried out in the following steps:

- Identifying the important process control variables.
- Selection of the useful limits of the welding parameters,viz. open-circuit voltage (V), current (A), travelling speed (S), and nozzle to plate distance (N).
- Developing the design matrix.
- Conducting the experiment as per design matrix.
- Recording the responses viz. penetration(P),bead width (w) & reinforcement height (H).
- Development of mathematical models.
- Calculating the co-efficient of polynomial.
- Checking adequacy of the models developed.
- Testing the significance of regression co-efficient recalculating the value of significant coefficient and arriving at the final mathematical models.
- Presenting the main effects and the significant interaction in 2D and 3D (contour) graphical form.
- Prediction of results using feed forward back propogation.
- Analysis of results and conclusion.

3.3.3.1 Identifying the important process control variables:

To predict weld bead dimensions and shape relationships, welding variables were identified to develop mathematical models. These included independently controllable welding process parameters like arc voltage (V), current /wire feed rate (A), travelling speed/welding speed (S) and nozzle-to-plate distance (N). The weld bead geometry and shape relationship chosen for this study were penetration (p), weld bead width (w), reinforcement height

(h). Therefore it was decided to take all these parameters in to account to design the experiments. Since the number of variables is less, and in order to determine more accurate relationships of the input–output variables, a full factorial design is chosen as the factorial portion of CCD. In general, a is chosen between 1 and K1/2, where K is the number of input parameters. The value of a is selected as 1.0 in the present investigation for the following reasons:

1. It makes the CCD possible by setting each input parameter at its three levels only.
2. If the value of a is large, the star points will be too far from the centre point, resulting in an improper design of the experiments.

As a rule of thumb, 3–5 runs are taken at the centre point. As the value of a is selected as 1.0 (i.e. the lower value of its range), the number of runs at the centre point is chosen as 3, in order to stabilize the prediction variance

3.3.3.2 Selection of the useful limits of the welding parameter:

Trials runs were carried out by varying one of the process parameters whilst keeping the rest of them at constant values. the working range was decided upon by inspecting the bead for smooth appearance and the absences of any visible defects. The upper limit of a factor was coded as +1 and lower limit as -1.

$$X_i = \frac{2\,[\,2X - (X_{max} + X_{min})\,]}{(X_{max} - X_{min})}$$

Where Xi = required coded value of a variable X

X = any value of the variable from X_{max} to X_{min}

X_{max} = upper level of the variable

X_{min} = lower level of the variable

i = number of parameter

The selected process parameters with their limits, units and notation are given in table3.3

				Level		
S.No.	**Parameters**	**Units**	**Notation**	**High (+1)**	**Middle(0)**	**Low(-1)**
1	**Current**	**Amp**	**A**	450	400	300
2	**Voltage**	**volts**	**V**	28	24	22
3	**Travelling Speed**	**mm/sec**	**S**	10	8.2	6
4	**Nozzle to plate distance**	**mm**	**N**	35	30	25

Table 3.3 Process control parameters and their Level

3.3.3.3 Developing the design matrix:

Weld no.	Trial no.	Input parameters			
		V	A (F)	S	N
1	10	-1	-1	-1	-1
2	12	+1	-1	-1	-1
3	5	-1	+1	-1	-1
4	23	+1	+1	-1	-1
5	14	-1	-1	+1	-1
6	19	+1	-1	+1	-1
7	11	-1	+1	+1	-1
8	25	+1	+1	+1	-1
9	2	-1	-1	-1	+1
10	24	+1	-1	-1	+1
11	13	-1	+1	-1	+1
12	22	+1	+1	-1	+1
13	7	-1	-1	+1	+1
14	20	+1	-1	+1	+1
15	1	-1	+1	+1	+1
16	21	+1	+1	+1	+1
17	15	0	0	0	0
18	6	-1	0	0	0
19	27	+1	0	0	0
20	26	0	-1	0	0
21	4	0	+1	0	0
22	17	0	0	0	0
23	9	0	0	-1	0
24	18	0	0	+1	0
25	3	0	0	-1	0
26	16	0	0	0	+1
27	8	0	0	0	0

Table 3.4 Design matrix

The design matrix, shown in table 3.4, is a central composite design consisting of 27 sets of coded condition.

Salient features of Design Matrix table are:

Trials indicate the sequence number of run under consideration. The signs +1 and -1 as already indicated refer to the upper and lower levels of that parameter under which they are recorded.

3.3.3.4 Conducting the experiments as per designed matrix

3.3.3.4.1 Welding Equipment

Machine used in Welding Laboratory, Delhi College of Engineering, Delhi.

Manufacture by: -- Quality Engineer (Baroda Pvt. Ltd.), A/18, Gujarat Estate, Dharamsingh Desai Marg, Chhani Road Baroda -390002

Machine Model: -- QSW800

Fig 3.14 Picture of SAW machine used for experimental work courtesy Quality Engineers.

Supply voltage: -- 380/440 Phase Three

Frequency: -- 50 Hz Operating voltage: -- 26- 60 Volts

Range of Welding: -- 800 Amp. O.C.V. Of Rectifier: -- 10-52 Volts

Maximum Welding Current at 100% duty cycle: -- 900 Amp

3.3.3.4.2 Base Metal

For carrying out research work , test specimen were prepared from 12 mm thickness Mild steel plate. Dimension of each plate were 254x76x12mm. Composition of the base material as supplied by the supplier was as follows:

C	S	Mn	S	Cr	Ni
0.102%	0.179%	0.466%	0.0705%	0.036	0.022

3.3.3.4.3 Consumables:

3.3.3.4.3.1 Wire:

3.2 mm diameter copper coated mild steel wire manufactured by (ESAB INDA LTD) was used specification of filler wire used was (AWS-A5.17 EL-8).

The chemical composition of filler wire was:

C	Mn	Si
0.10%	0.45%	0.02%

3.3.3.4.2 Flux

The study was carried out by using available flux i.e. an agglomerated Flux Manufactured by ESAB INDIA LTD.

The specification of the flux was:

Automelt Gr.II, Coding - AWS / SFA 5.17

F7AZ - EL8

F7PZ - EL8

The Chemical Composition was:

C	Mn	Sn
0.08%	1.00%	0.25%

3.3.3.4.3 Experimental Procedure The experiment has been performed on constant voltage fully automatic submerged arc welding machine of 800 A, 380/440/3-phase .50 H z rectifier type power source, 3.2mm copper coated mild steel electrode **.** Welding was carried out in single pass by using bead-on-plate technique. Weld beads were deposited as per condition dicted by the design matrix. In 27 trials, beads were laid on 27 plates.

Two specimens of 16mm width were cut transverse to the weld bead from each welded plates. These specimens were ground, polished and etched with 2% nital (98% alcohol + 2% of nitric acid). All specimens of first set were macro etched for reveal the bead profile and some specimens of second set were micro etched for reveal microstructure.

Weld bead profiles were traced by using an optical profile projector/Image analysis and bead dimensions viz., penetration (p), width (w) and reinforcement (h) were measured. The average bead dimensions and shape relationships were given in table3.5

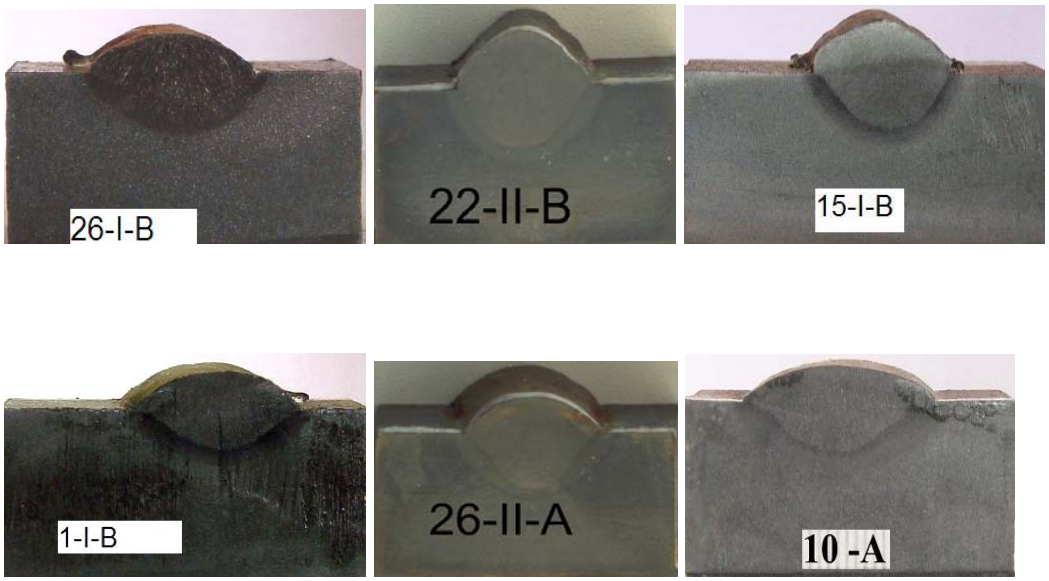

Fig 3.15 Picture of Bead shape from experiments conducted on SAW

3.3.3.5 Recording the responses:

Weld no.	Trial no.	Input parameters				Responses		
		V	A (F)	S	N	Bead Height	Bead Width	Penetration
1	10	-1	-1	-1	-1	1.5	11.1	3.2
2	12	1	-1	-1	-1	1.9	14.1	5.1
3	5	-1	1	-1	-1	3.1	11.1	3.7
4	23	1	1	-1	-1	2.2	13	7.2
5	14	-1	-1	1	-1	1.2	10.7	2.4
6	19	1	-1	1	-1	3.1	10.8	2.6
7	11	-1	1	1	-1	2.8	10.6	3.7
8	25	1	1	1	-1	1.8	11.4	5.1
9	2	-1	-1	-1	1	2.8	9.5	2.4
10	24	1	-1	-1	1	1.8	12.8	3.7
11	13	-1	1	-1	1	5.7	9.5	3.2
12	22	1	1	-1	1	3.5	12.8	6.2
13	7	-1	-1	1	1	2.2	9	3.2
14	20	1	-1	1	1	2.5	10.1	3
15	1	-1	1	1	1	4.8	9.2	4
16	21	1	1	1	1	2.5	9	5.6
17	15	0	0	0	0	2.8	10.6	4
18	6	-1	0	0	0	3	8.4	2
19	27	1	0	0	0	2.2	11.1	3.4
20	26	0	-1	0	0	1.2	10.6	3.7
21	4	0	1	0	0	3.8	10.7	7.6
22	17	0	0	0	0	2.8	10.7	3.7
23	9	0	0	-1	0	3.1	11.7	5
24	18	0	0	1	0	1.9	11.3	3.2
25	3	0	0	-1	0	1.2	10.2	4.8
26	16	0	0	0	1	4.8	10.7	3.4
27	8	0	0	0	0	2.6	10.8	3.4

Table 3.5 Observed values of bead parameters

Chapter – 4

DEVELOPMENT OF MATHEMATICAL MODELS

4.0 DEVELOPMENT OF MATHEMATICAL MODELS

4.1 Introduction

Mathematical models can be proposed as the basis for a control system for the SAW process to predict particular weld bead geometry and to establish the interrelationship between weld process parameters to weld bead geometry. The experimental data were used to develop nonlinear models, and analysis of the models was carried out through ANOVA and surface plots. Minitab15 software was used for this purpose.

4.2 Development of a mathematical model

The response function representing any of the weld-bead dimensions can be expressed as :

$$Y. = f(V, A, S, N) \qquad (4.1)$$

where, Y= Weld bead response

V= Arc voltage

A= Current

S= Welding speed

N= Nozzle-to-plate distance.

The relationship selected being a second-degree response surface expressed as follows:

$$Y=b_0+b_1V+b_2A+b_3S+b_4N+b_{11}V^2+b_{22}A^2+b_{33}S^2+b_{44}N^2+b_{12}VA+b_{13}VS$$
$$+b_{14}VN+b_{23}AS+b_{24}AN+b_{34}SN. \qquad (4.2)$$

Where $b_{0,}$ is constant and $b_{1,}$ $b_{2,}$ $b_{3,}$ $b_{4,}$ $b_{11,}$ $b_{22,}$ $b_{33,}$ $b_{44,}$$b_{12,}$ $b_{13,}$ $b_{14,}$ $b_{23,}$ $b_{24,}$ b_{34} are co-efficient of the model.

4.3 Evaluation of the co-efficient of the model

The values of the coefficients of the polynomial of equation (4.1) were calculated by the regression method. The Minitab (15.0 version) software package was used to calculate the values of these coefficients for different responses.

4.3.1 Response: Bead Height

Bead height was expressed as a non–linear function of the input process parameters (in coded form) as follow as :

$$\text{Bead Height} = 2.83 - 0.311\,V + 0.67\,A - 0.11\,S + 0.52\,N - 0.5\,V*A + 0.16\,V*S - 0.35\,V*N - 0.23\,A*S + 0.31\,A*N - 0.13\,S*N - 0.27\,V^2 - 0.37A^2 - 0.83\,S^2 + 1.36\,N^2 \quad (4.3)$$

4.3.2 Response: Bead Width

Bead width was expressed as a non–linear function of the input process parameters (in coded form) as follow as :

$$\text{Bead Width} = 10.6 + 0.89\,V - 0.08\,A - 0.68\,S - 0.69\,N - 0.11\,V*A - 0.61\,V*S + 0.11\,V*N + 0.04\,A*S - 0.02\,A*N - 0.09\,S*N - 0.84\,V^2 + 0.06\,A^2 + 0.24\,S^2 + 0.83\,N^2 \quad (4.4)$$

4.3.2 Response: Penetration

Penetration was expressed as a non–linear function of the input process parameters (in coded form) as follow as :

$$\text{Penetration} = 3.87 + 0.78\,V + 0.94\,A - 0.4\,S - 0.1\,N + 0.39\,V*A - 0.42\,V*S - 0.08\,V*N + 0.08\,A*S + 0.02\,A*N + 0.36\,S*N - 1.26\,V^2 + 1.69\,A^2 + 0.27\,S^2 - 0.55\,N^2 \quad (4.5)$$

Estimated value of the coefficients of the model is shown in table 4.1

S.No.	Coefficient	Reinforcement Height (H)	Width (W)	Penetration (P)
1	b0	2.83	10.63	3.87
2	b1	-0.31	0.89	0.78
3	b2	0.67	-0.08	0.94
4	b3	-0.11	-0.68	-0.40
5	b4	0.52	-0.69	-0.10
6	b11	-0.27	-0.84	-1.26
7	b22	-0.37	0.06	1.69
8	b33	-0.83	0.24	0.27
9	b44	1.36	0.83	-0.55
10	b12	-0.50	-0.11	0.39
11	b13	0.16	-0.61	-0.42
12	b14	-0.35	0.11	-0.08
13	b23	-0.23	0.04	0.08
14	b24	0.31	-0.02	0.02
15	b34	-0.13	-0.09	0.36

Table 4.1 Estimated value of the coefficients of the model

4.4 Checking adequacy of the model

The analysis of variance (ANOVA) technique was used to check the adequacy of the developed models. As per this technique,

(a) The F-ratio of the developed model is calculated and is compared with the standard tabulated value of F-ratio for a specific level of confidence ,

(b) If calculated value of F-ratio does not exceed the tabulated value, then with the corresponding confidence probability the model may be considered adequate.

The F-ratio of the model is defined as the ratio of variation between the samples (MSC) to the variation within the samples (MSE). Therefore:

F_{model} = Variation between the samples / Variation within the samples.

Source of variation	Sum of squares	Degree of Freedom	Mean squares	Variance ratio (f-ratio)
Between Columns	SSC	(c-1)	MSC = SSC/(r-1)	MSC/MSE
Between Rows	SSR	(r-1)	MSR = SSR/(r-1)	MSR/MSE
Residual or error	SSE	(c-1) (r-1)	MSE= SSE/(c-1) (r-1)	
Total	SST	(n-1)		

Table 4.2 General ANOVA table.

where

SSC = Sum of squares between columns

SSR = Sum of squares between rows

SSE = Sum of squares due to error

SST = Total sum of squares

MSC = Mean square between columns

MSR = Mean square between rows

MSE = Mean square error

F = Ratio of MSC to MSE or Ratio of MSC to MSE

4.4.1 ANOVA for Response Surface Quadratic Model

4.4.1.1. Response: - Bead Height

Source	Sum of Squares	df	Mean Square	F Value	p-value Prob > F	
Model	28.82	14	2.06	7.29	0.0007	Significant
A-V	1.74	1	1.74	6.17	0.0287	
B-A	8.00	1	8.00	28.34	0.0002	
C-S	0.21	1	0.21	0.73	0.4087	
D-N	4.35	1	4.35	15.40	0.002	
AB	4.00	1	4.00	14.17	0.0027	
AC	0.42	1	0.42	1.50	0.2447	
AD	1.96	1	1.96	6.94	0.0218	
BC	0.81	1	0.81	2.87	0.1161	
BD	1.56	1	1.56	5.53	0.0365	
CD	0.25	1	0.25	0.89	0.3653	
A^2	0.18	1	0.18	0.62	0.4449	
B^2	0.33	1	0.33	1.17	0.3014	
C^2	1.98	1	1.98	7.01	0.0213	
D^2	3.01	1	3.01	10.65	0.0068	
Residual	3.39	12	0.28			Not Significant
Lack of Fit	1.56	9	0.17	0.28	0.9384	
Pure Error	1.83	3	0.61			
Total	32.21	26				

Table 4.3 ANOVA table for Bead height.

The Model F-value of 7.29 implies the model is significant. There is only a 0.07% chance that a "Model F-Value" this large could occur due to noise. Values of "Prob > F" less than 0.0500 indicate model terms are significant. In this case A, B, D, AB, AD, BD, C^2, D^2 are significant model terms. Values greater than 0.1000 indicate the model terms are not significant.The "Lack of Fit F-value" of 0.28 implies the Lack of Fit is not significant relative to the pure error.Non-significant lack of fit is good -- we want the model to fit.

4.4.1.2. Response: - Bead Width

Source	Sum of Squares	df	Mean Square	F Value	p-value Prob > F	
Model	39.43	14	2.82	6.52	0.0012	Significant
A-V	14.22	1	14.22	32.92	< 0.0001	
B-A	0.11	1	0.11	0.25	0.6247	
C-S	8.53	1	8.53	19.74	0.0008	
D-N	7.61	1	7.61	17.62	0.0012	
AB	0.18	1	0.18	0.42	0.5301	
AC	5.88	1	5.88	13.61	0.0031	
AD	0.18	1	0.18	0.42	0.5301	
BC	0.03	1	0.03	0.07	0.7946	
BD	0.01	1	0.01	0.01	0.9110	
CD	0.14	1	0.14	0.33	0.5788	
A^2	1.68	1	1.68	3.89	0.0722	
B^2	0.01	1	0.01	0.02	0.8927	
C^2	0.16	1	0.16	0.38	0.5483	
D^2	1.12	1	1.12	2.59	0.1336	
Residual	5.18	12	0.43			
Lack of Fit	4.04	9	0.45	1.18	0.4994	Not Significant
Pure Error	1.15	3	0.38			
Total	44.61	26				

Table 4.4 ANOVA table for Bead width.

The Model F-value of 6.52 implies the model is significant. There is only a 0.12% chance that a "Model F-Value" this large could occur due to noise. Values of "Prob > F" less than 0.0500 indicate model terms are significant. In this case A, C, D, AC are significant model terms. Values greater than 0.1000 indicate the model terms are not significant. The "Lack of Fit F-value" of 1.18 implies the Lack of Fit is not significant relative to the pure error. Non-significant lack of fit is good -- we want the model to fit

4.4.1.3. Response: - Penetration

Source	Sum of Squares	df	Mean Square	F Value	p-value Prob > F	
Model	47.35	14	3.38	11.68	< 0.0001	Significant
A-V	11.05	1	11.05	38.14	< 0.0001	
B-A	16.06	1	16.06	55.44	< 0.0001	
C-S	2.96	1	2.96	10.21	0.0077	
D-N	0.15	1	0.15	0.51	0.4889	
AB	2.48	1	2.48	8.57	0.0127	
AC	2.81	1	2.81	9.69	0.0090	
AD	0.11	1	0.11	0.36	0.5571	
BC	0.11	1	0.11	0.36	0.5571	
BD	0.01	1	0.01	0.02	0.8915	
CD	2.03	1	2.03	7.01	0.0213	
A^2	3.75	1	3.75	12.96	0.0036	
B^2	6.79	1	6.79	23.45	0.0004	
C^2	0.21	1	0.21	0.74	0.4067	
D^2	0.49	1	0.49	1.68	0.2191	
Residual	3.48	12	0.29			
Lack of Fit	3.28	9	0.36	1.04	0.5248	Not Significant
Pure Error	0.20	3	0.07			
Total	50.82	26				

Table 4.5 ANOVA table for Penetration.

The Model F-value of 11.68 implies the model is significant. There is only a 0.01% chance that a "Model F-Value" this large could occur due to noise. Values of "Prob > F" less than 0.0500 indicate model terms are significant. In this case A, B, C, AB, AC, CD, A^2, B^2 are significant model terms. Values greater than 0.1000 indicate the model terms are not significant. The "Lack of Fit F-value" of 1.04 implies the Lack of Fit is not significant relative to the pure error. Non-significant lack of fit is good -- we want the model to fit.

4.4.2 Calculation of Variance for testing the adequacy of the models :

Bead geometry parameters	First-order terms		Second-order terms		Lack of fit		Error term		F-ratio	Whether the model is adequate
	(S.S)	(df)	(S.S)	(df)	(S.S)	(df)	(S.S)	(df)		
Height	16.10	4	12.73	10	1.6	9	1.8	3	0.28	Adequate
Width	30.20	4	9.22	10	4.04	9	1.1	3	1.18	Adequate
Penetration	30.53	4	16.82	10	3.27	9	0.2	3	5.46	Adequate

Table 4.6 Results of calculations ANOVA table

Table 4.6 shows the results of the calculation of variance for testing the adequacy of the models. The different terms used in table are as follows: The term 'S.S' stands for the sum of squares. The term 'df' indicates degree of freedom. $F\text{-ratio}_{(10,\ 3,0.05)} = 8.78$.

4.5 Development of the final models.

The models developed to predict the weld bead geometry relationship are as follows:

$$\text{Bead Height} = 2.83 - 0.311\ V + 0.67\ A + 0.52\ N - 0.5\ V*A - 0.35\ V*N + 0.31\ A*N - 0.83\ S^2 + 1.36\ N^2. \quad (4.6)$$

$$\text{Bead Width} = 10.6 + 0.89\ V - 0.68\ S - 0.69N - 0.61\ V*S. \quad (4.7)$$

$$\text{Penetration} = 3.87 + 0.78\ V + 0.94\ A - 0.4\ S + 0.39\ V*A - 0.42\ V*S + 0.36\ S*N - 1.26\ V^2 + 1.69\ A^2 . \quad (4.8)$$

4.6 Testing of the models

The models were also tested for some test cases (table 4.6). Seven cases were generated, at random, by considering different combinations of the input variables (lying within their respective ranges), and for each combination the outputs were determined experimentally. The results are shown in table 4.7 . The model-predicted permeability values were compared with their respective experimental values (Fig. 4.1(a, b & c)).The best –fit line of these points was found to be close to the ideal y=x line. This indicate that the model is able to make the predictions accurately.

Weld No.	V (volts)	A (amp)	S (mm/sec)	N (mm)		Bead Height	Bead Width	Penetration
3	22	450	6	25	Actual	3.2	11.1	3.8
					Predicted	3.7	10.7	4.0
					Error %	14.41	3.60	5.26
6	28	300	10.7	25	Actual	3.2	10.8	2.7
					Predicted	3.0	10.9	2.5
					Error %	5.66	-0.79	7.41
9	22	300	6	35	Actual	2.7	9.5	2.5
					Predicted	3.1	9.1	2.8
					Error %	13.37	4.26	12.00
17	24	400	8.3	30	Actual	2.7	10.6	4.5
					Predicted	2.8	10.6	4.1
					Error %	4.81	0.00	8.89
21	24	450	8.3	30	Actual	3.7	10.7	7.4
					Predicted	3.5	10.6	7.1
					Error %	5.41	0.93	4.05
22	24	400	8.3	30	Actual	2.7	10.7	3.8
					Predicted	2.8	10.6	3.9
					Error %	4.81	0.93	1.84
26	24	400	8.3	35	Actual	4.7	10.2	3.5
					Predicted	4.7	9.9	3.8
					Error %	0.21	2.84	8.57

Table 4.7 Input – output data of the test cases.

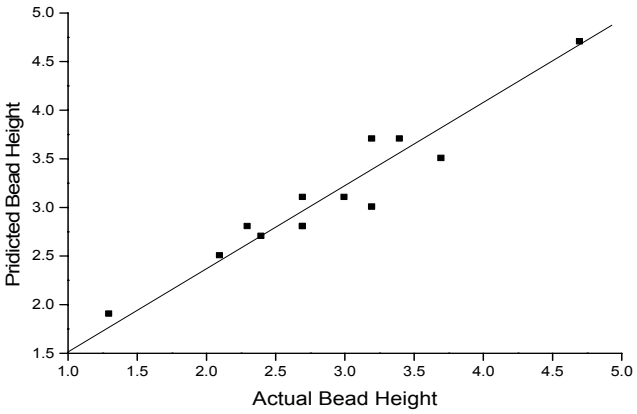

Fig 4.1 (a)

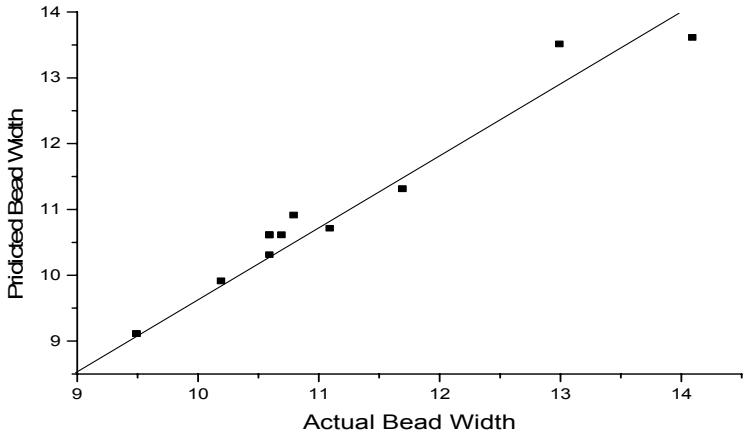

Fig 4.1 (b)

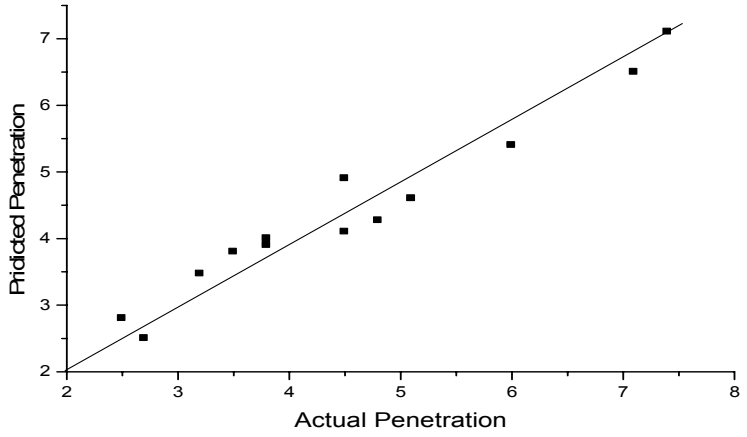

Fig 4.1 (c)

Fig 4.1 Comparison of Actual vs. Predicted values of test cases

Chapter - 5

RESULTS AND DISCUSSIONS

5.0 RESULTS AND DISCUSSIONS

5.1 Direct effects of process parameters

It is observed from fig. 5.1 indicates that penetration (*P*) and bead width (*W*) increase, but bead height (H) decreases with increase in voltage (*V*). These effects are due to the following reason: the increase in voltage (V) results in increase in the arc length, arc voltage and heat input, but it has little influence on the wire fusion speed. The increase in the heat input results in increase in penetration (P). The increase in the arc length results in the spreading of arc cone at its base which leads to an increase in bead width (W). The marginal increase in the heat input and the metal deposition rate are utilized for increasing the value of P and so the bead height H decreases with increase in voltage (V).

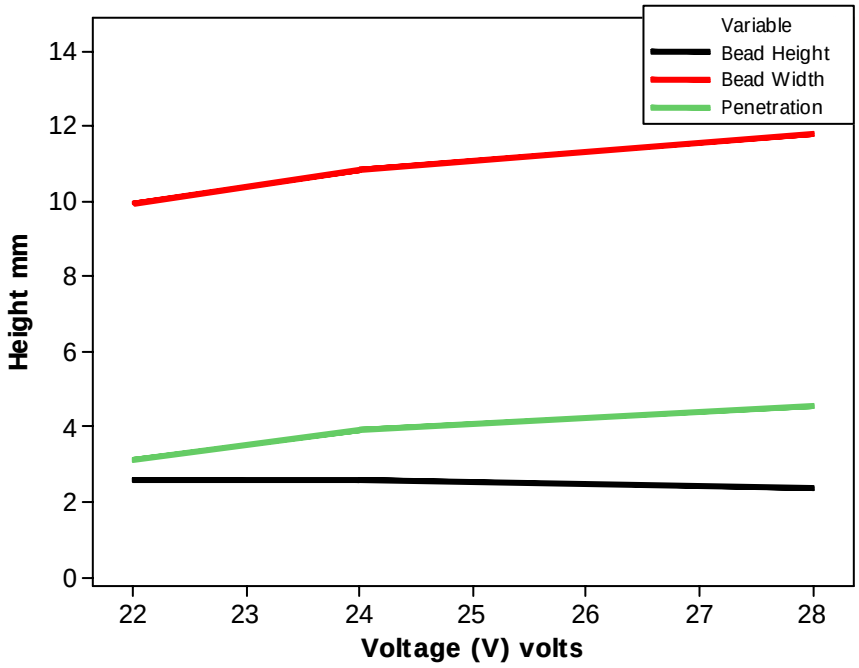

Fig. 5.1 Effect of voltage on Bead parameters.

Fig. 5.2 indicates that penetration (P) and bead height (H) increases with increases in current (A). The value of bead width (W) remains unaltered by the increase of current (A). These effects are due to the following reason: with increase in current (A), heat input per unit time and the weight of wire fused and deposited per unit time increases. Therefore the size of the weld pool increases. Hence penetration (P) and bead height (H) increases. However there is no change in the cross-section of the arc cone and so the value of bead height (H) is unaltered by current (A).

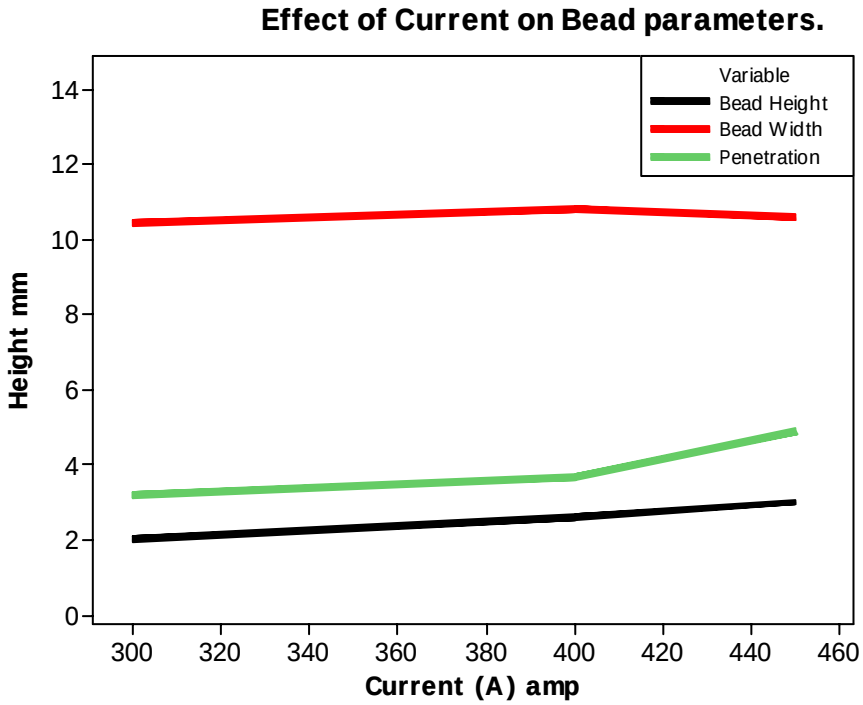

Fig. 5.2 Effect of Current on Bead parameters.

From fig. 5.3 it is noted that all the factors viz. penetration (*P*), bead width (*W*) and bead height (H) decreases with increase in welding speed (S). These effects are due to the welding torch travelling at high speed over the base metal when *S* is increased. This increase in torch speed leads to lesser metal deposition rate on the bead. Also the increase in welding speed (S) reduces

the heat input and hence the weight of base metal melted. Because of less heat input and a lesser metal deposition rate, the size of weld pool reduces and hence all of the bead factors reduce with increase in welding speed (S).

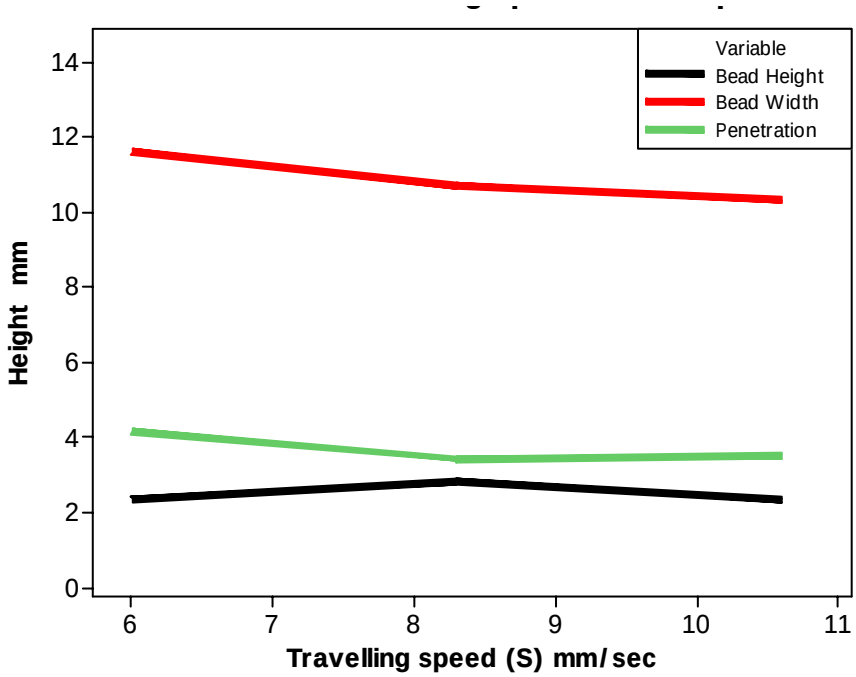

Fig 5.3 Effect of Travelling sped on Bead parameters.

From fig. 5.4, it is evident that as the nozzle-to-plate distance (N) increases, penetration (*P*) and bead width (*W*) reduce but bead height (H) increases. These effects are due to the following: the welding current and heat input decrease with increase in N. Because of the reduced heat input the value of P and W reduce but the metal fusion rate increases at higher value of N because of the Joule heating effect. Hence H increases with increase in N. As both P and W decrease with increase in N, the area of penetration.

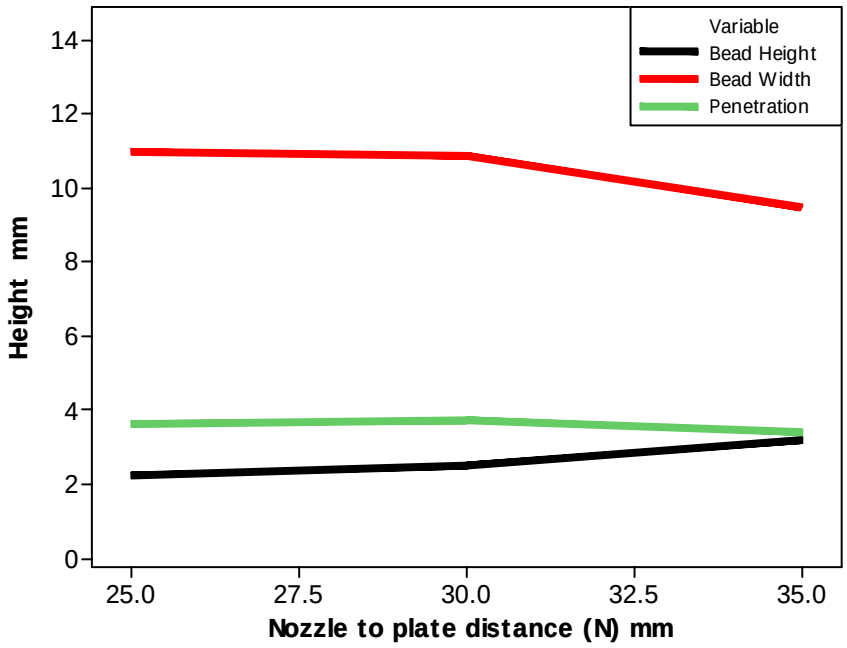

Fig 5.4 Effect of Nozzle to plate distance on Bead parameters.

5.2 Interaction effects of process parameters.

5.2.1. Interaction effect of Voltage and Current on Penetration.

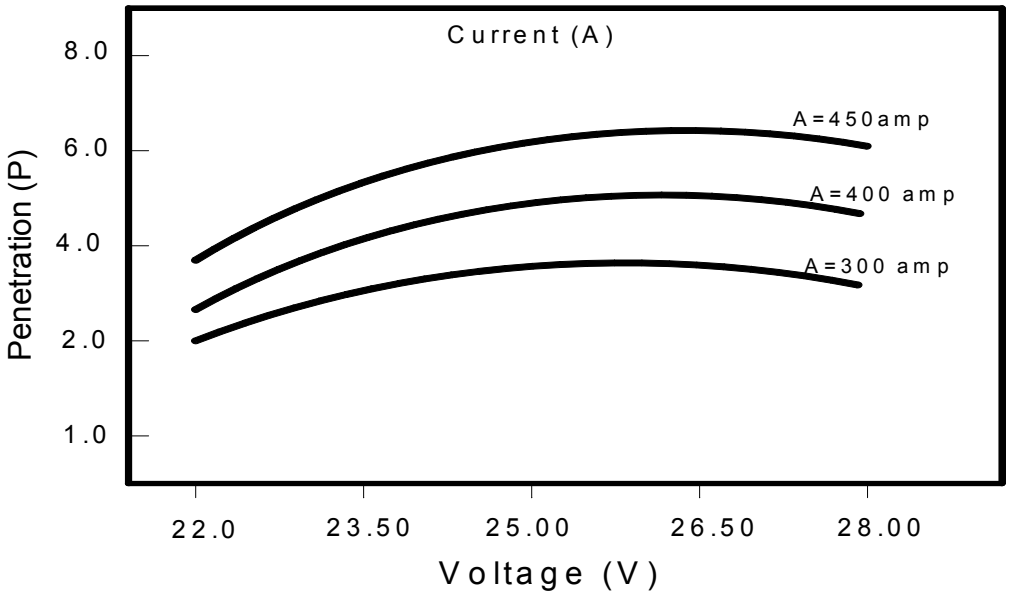

Fig 5.5 Interaction effect of Voltage and Current on Penetration.

Fig. 5.5 indicates that the penetration (P) increases with increase in current (A). It also increases with increase in voltage (V). This is because both V and F have positive effects on P. Hence the increasing trend of P with increase

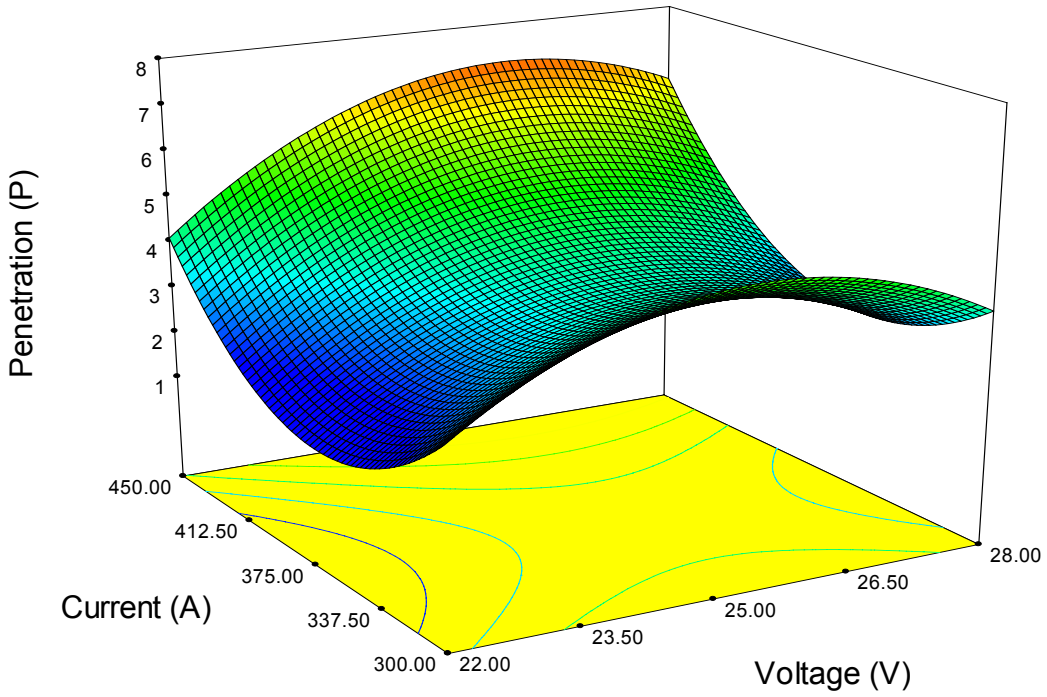

Fig 5.6 Surface & contour plot showing interaction effect of V and C on P.

in V gradually decreases with decrease in A. These effects are more clear from fig. 5.6, which shows the contour graph of P. From this graph it is noted that P is maximum when A is at 450 amps. Whilst V is between the 25 v and 27 v but increases further with further increase in V.

5.2.2. Interaction effect of Voltage and Welding speed on Penetration.

It is evident from fig. 5.7 that penetration P increases with increase in voltage V, whereas it decreases with increase in welding speed S. These effects are due to V having a positive effect but S having a negative effect on *P*. Hence the increasing trend of P decreases with increase in S. These effects are

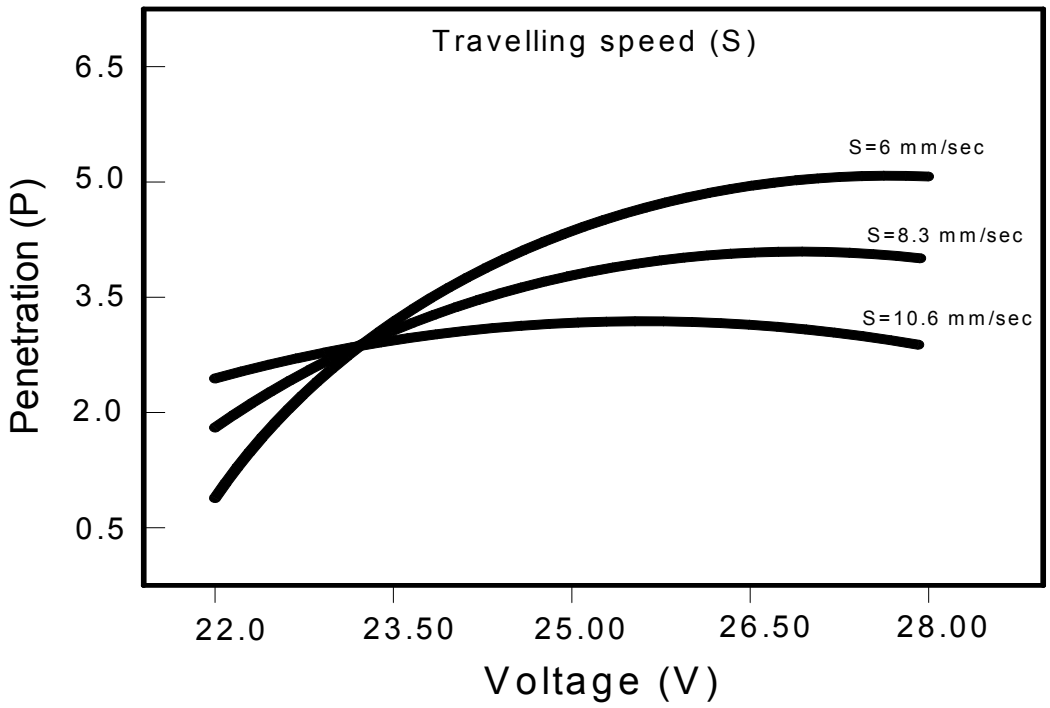

Fig 5.7 Interaction effect of Voltage and Welding speed on Penetration

further seen from fig. 5.8, which is the contour graph of *P*. From this graph, it is clear that *P* is maximum when S is at 6mm/sec with V is at 28v.

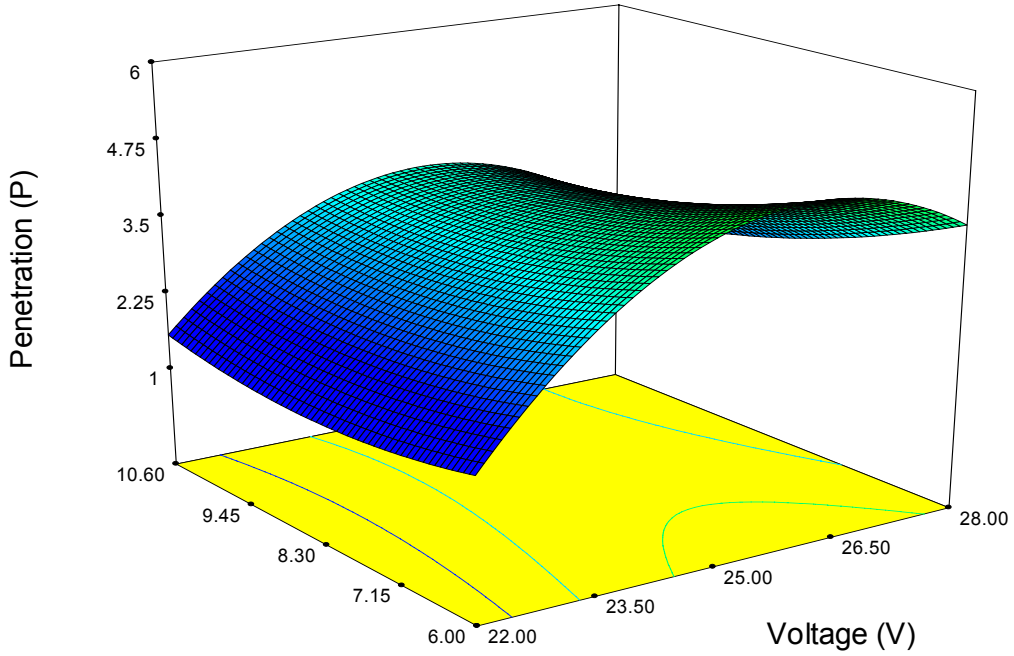

Fig 5.8 Surface & contour plot showing interaction effect of V and S on P.

5.2.3. Interaction effect of Voltage and Welding speed on Bead width.

Fig. 5.9 shows that the bead width (*W*) increases with increase in V. This increasing trend of *W* with increase in V gradually decreases with increase in S. This is because V has a positive effect whereas S has a negative effect on *W* and so the increasing trend of *W* with increase in *V* decreases with increase in *S*.

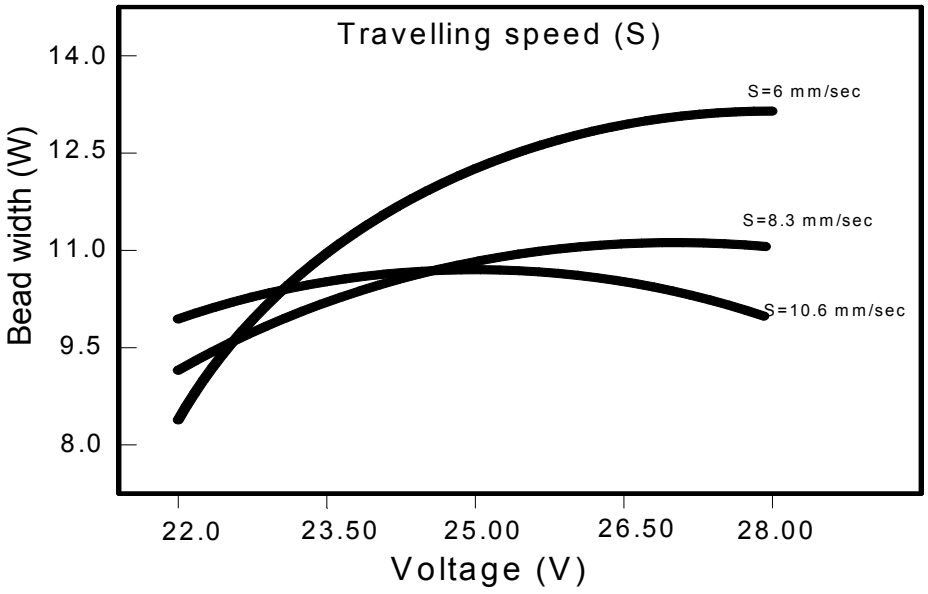

Fig 5.9 Interaction effect of Voltage and Welding speed on Bead width

These effects are further clarified in Fig. 5.10, which shows the contour graph of *W*. From this graph, it is noted that *W* is high when *V* is at 28 v with S is at 6 mm/sec.

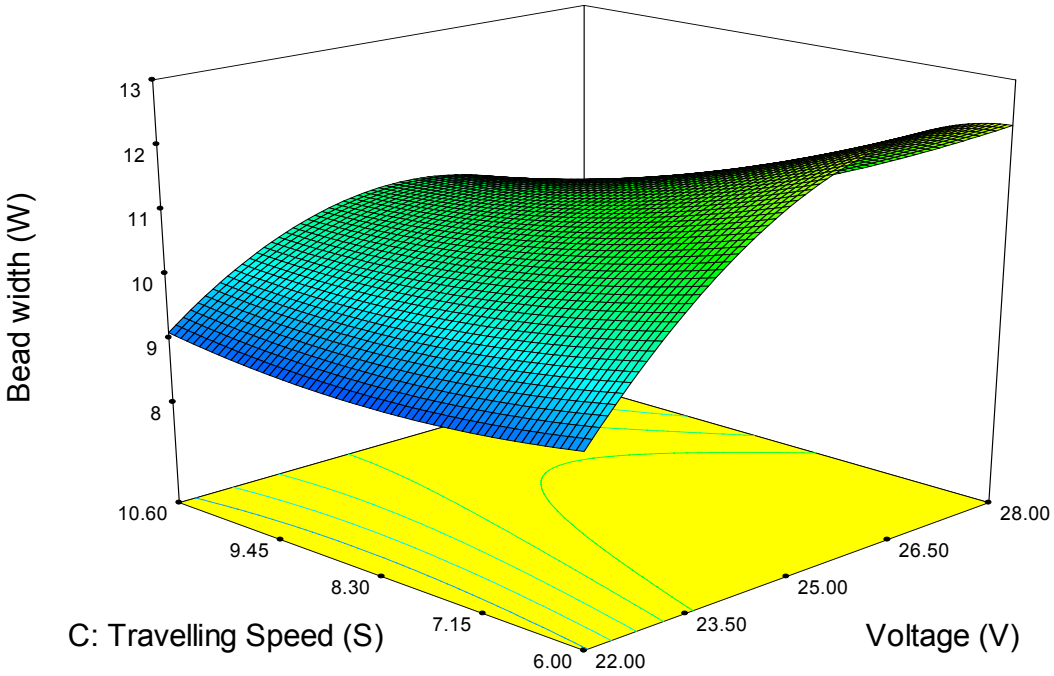

Fig 5.10 Surface & contour plot showing interaction effect of V and S on W.

5.2.4. Interaction effect of Current and Welding speed on Bead height.

It is apparent from fig. 5.11 that the bead height H increases with increase in the current A, but it decreases with increase in the welding speed S. These effects are due to A having a positive effect but *S* having a negative effect on H. Thus the increasing trend of H with increase in A decreases with increase in S. The contour graph of H shown in Fig. 5.12 also shows the same trend in which maximum value of *R* is obtained when A is at 450 amps with *S* at 6 mm/sec.

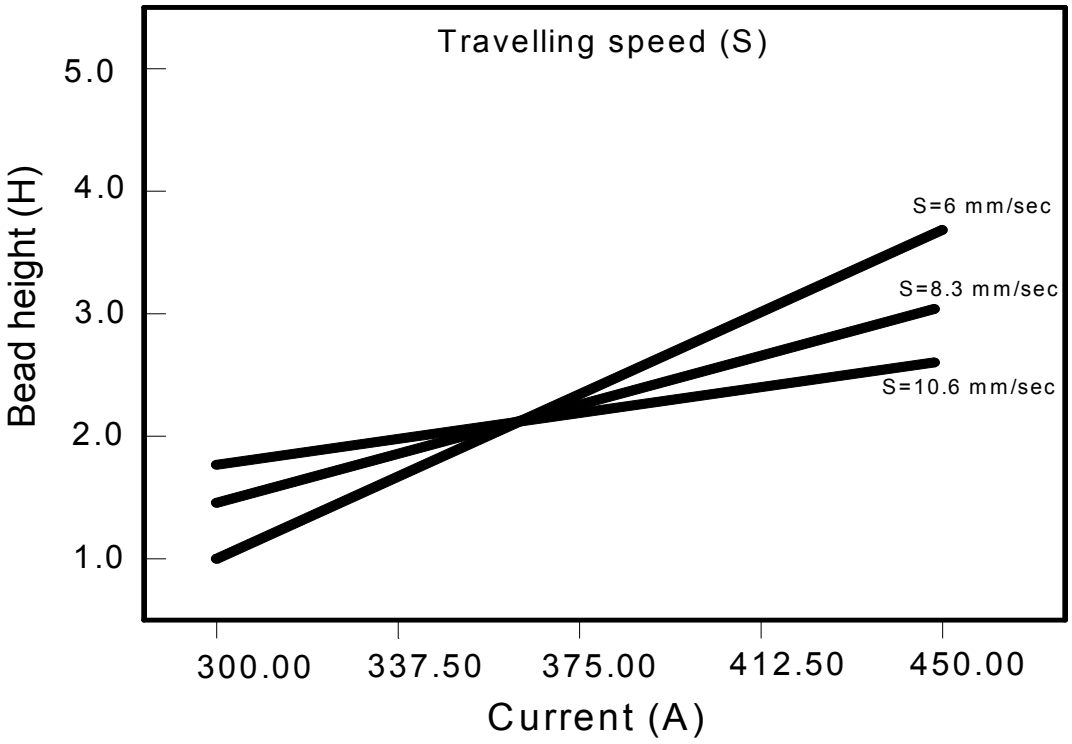

Fig 5.11 Interaction effect of Current and Welding speed on Bead height.

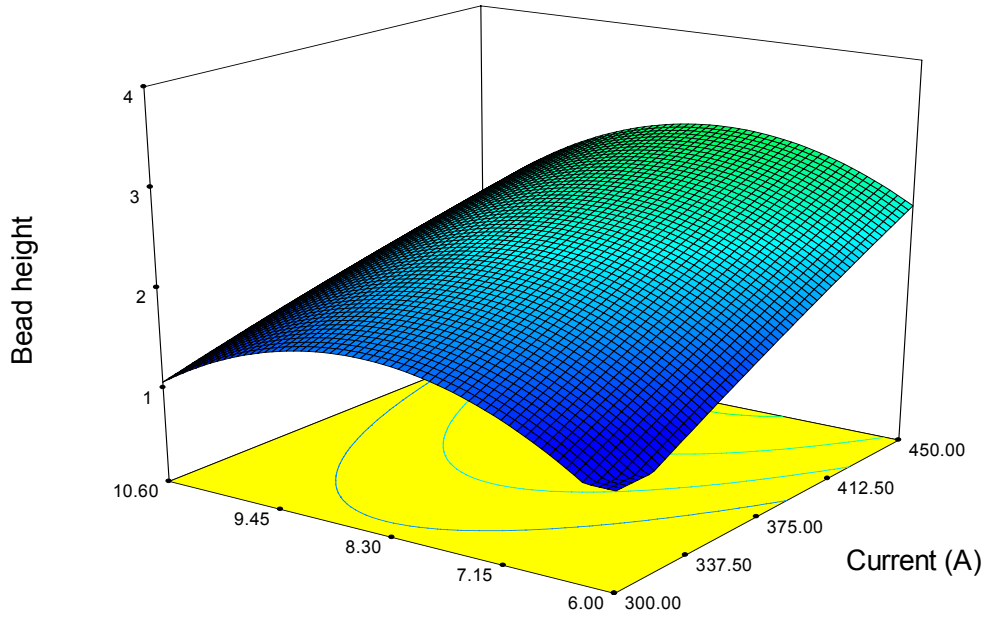

Fig 5.12 Surface & contour plot showing interaction effect of A and S on H.

5.2.5. Interaction effect of Current and Nozzle-to-plate distance on Bead height.

Fig. 5.13 indicates that the bead height (H) generally increases with increase in the current (A). It also increases with increase in the nozzle-to-plate distance N. The positive effects of both A and *N* are the reasons for the above effects on H.

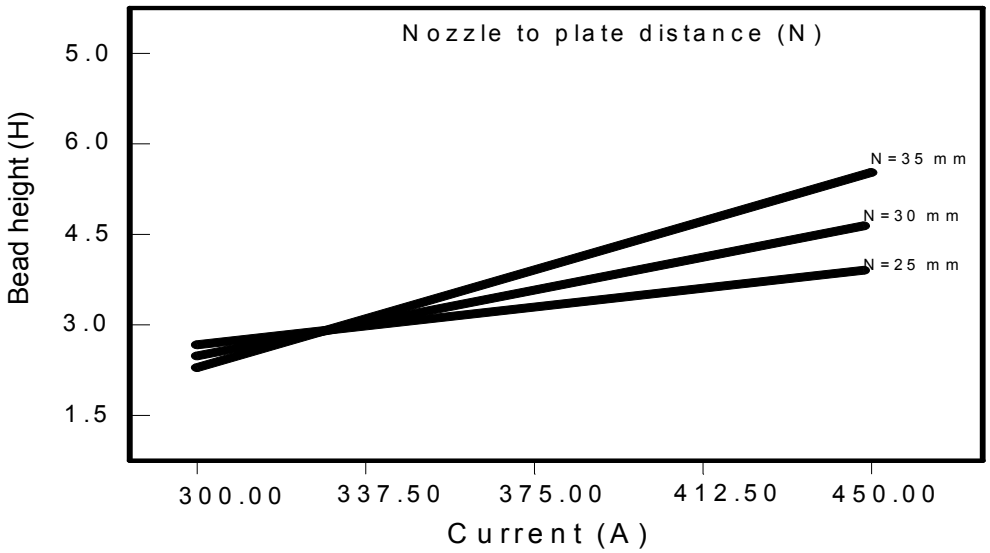

Fig. 513 Interaction effect of Current and Nozzle-to-plate distance on Bead height**.**

The contour graph of H shown in fig. 5.14 shows the same trend in which maximum value of H is obtained when A is at 450 amps and N is at 35mm.

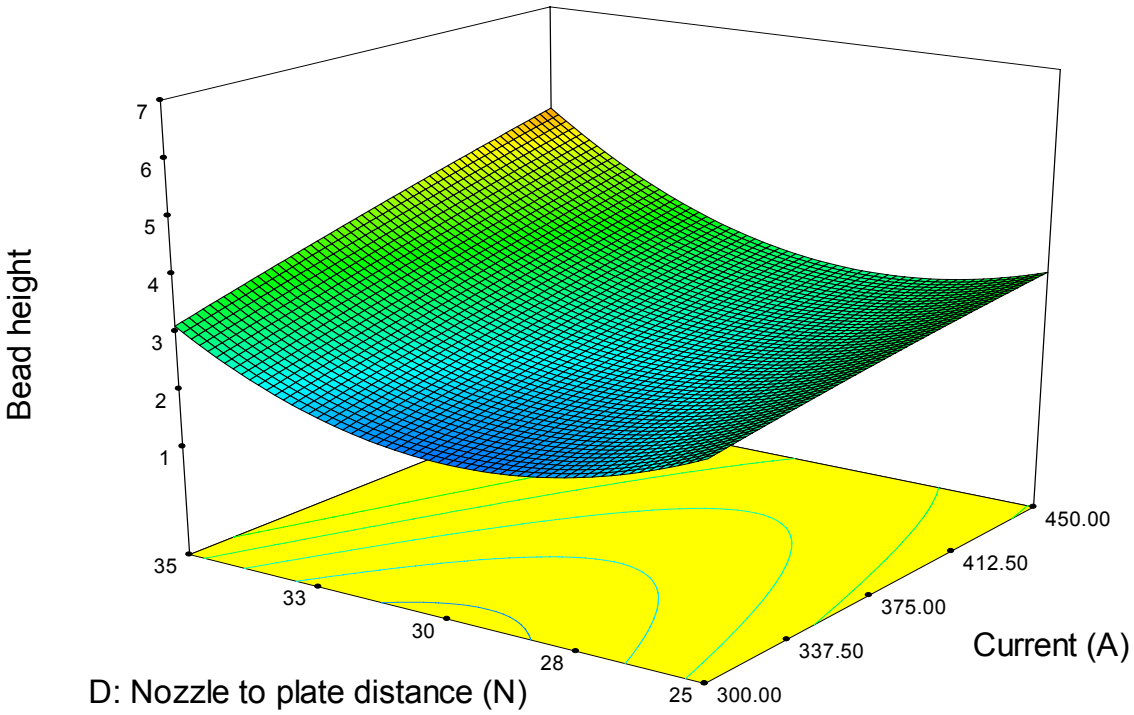

Fig 5.14 Surface & contour plot showing interaction effect of A and N on H.

Chapter - 6

MODELLING USING ARTIFICIAL NEURAL NETWORK (ANN)

6.0 MODELLING USING ARTIFICIAL NEURAL NETWORK (ANN).

6.1 Artificial Neural Network (ANN)

A neural network is an adaptable system that can learn relationships through repeated presentation of data and is capable of generalising to new, previously unseen data. If a network is to be of any use, there must be inputs (which carry the values of variables of interest in the outside world) and outputs (which form predictions, or control signals). Inputs and outputs correspond to sensory and motor nerves such as those coming from the eyes and leading to the hands. However, there may also be hidden neurones, which play an internal role in the network. The input, hidden and output neurones need to be connected together. To capture the essence of biological neural systems, an artificial neurone is used. It receives a number of inputs (either from original data, or from the output of other neurones in the neural network). Each input comes via a connection, which has a strength (or weight); these weights correspond to synaptic efficacy in a biological neurone. Each neurone also has a single threshold value. The weighted sum of the inputs is formed, and the threshold subtracted, to compose the activation of the neurone (also known as the post-synaptic potential, or PSP, of the neurone).

The activation signal is passed through an activation function (also known as a transfer function) to produce the output of the neurone. For our application, this function is a sigmoid function, which is the same for all neurones.

$$f(x) = \{1 + \exp(-x)\}^{-1}$$

The best-known example of a neural network training algorithm is back-propagation. In back propagation, the gradient vector of the error surface is calculated. This vector points in the direction of steepest descent from the current point, so we know that if we move along it a ‘‘short’’ distance, we will decrease the error. A sequence of such moves (slowing as we near the bottom) will eventually find a minimum of some sort. Large steps may converge more quickly, but may also overstep the solution or (if the error surface is very eccentric) go off in the wrong direction. A classic example of this in neural network training is where the algorithm progresses very slowly along a steep, narrow, valley, bouncing from one side across to the other. In contrast, very small steps may go in the correct direction, but they also require a large number of iterations. In practice, the step size is proportional to the slope (so that the algorithms settle down to a minimum) and to a special constant, the learning rate. The correct setting for the learning rate is application-dependent, and is typically chosen by experiment; it may also be time-varying, getting smaller as the algorithm progresses.

The algorithm progresses iteratively through a number of epochs. On each epoch, the training cases are each submitted in turn to the network, and target and actual outputs compared and the error calculated. This error, together with the error surface gradient, is used to adjust the weights, and then the process repeats. The initial network configuration is random, and training stops when a given number of epochs elapse, or when the error reaches an acceptable level, or when the error stops improving. We can select which of these stopping conditions to use.

A typical back-propagation network is shown in Fig. 6.1. Neurones are arranged in a distinct layered topology. The input layer is not really neural at all: these units simply serve to introduce the values of the input variables.

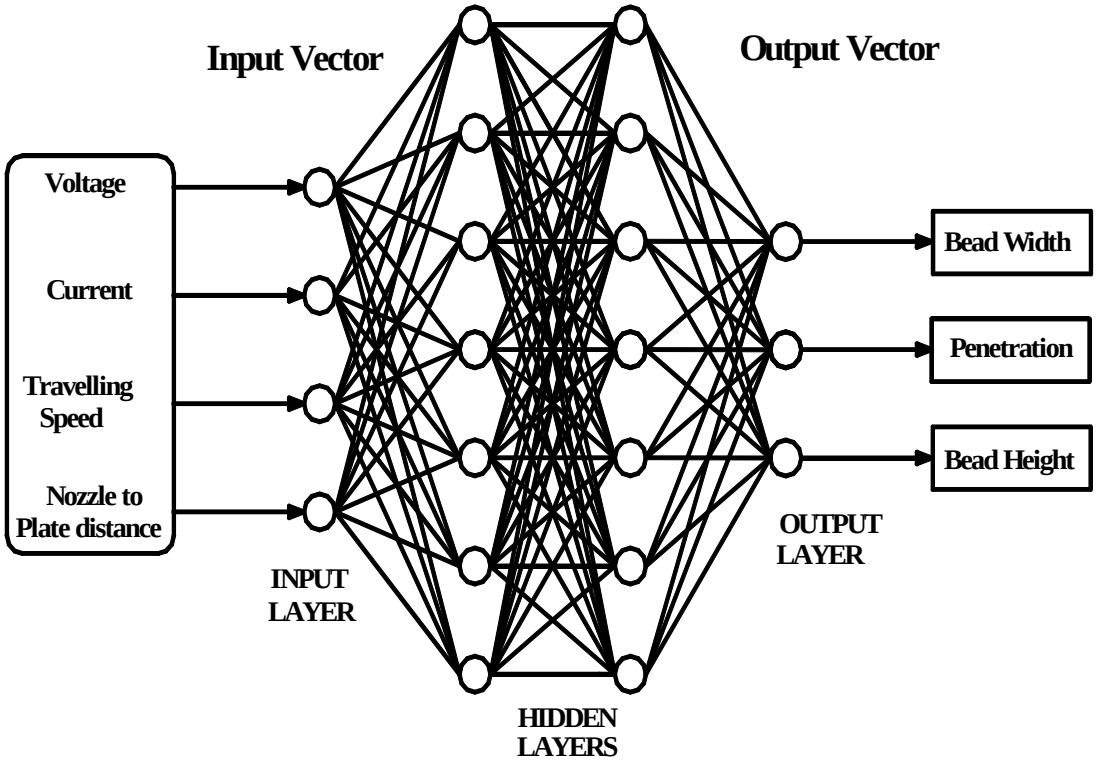

Fig 6.1 Back-propogation neural network used for predicting bead geometry.

6.2 Computational work

Several computational experiments were conducted, in the Software (Matlab), following are some of the observation:

6.2.1 Computational Experiment No. 1

Network Name: Ex-17

No. of Hidden Layers: 3

Network Type: Feed Forward Back Propogation

Training Function: Gradient descent with momentum back propagation

No. of Neurons in First Hidden Layer: 10

No. of Neurons in Second Hidden Layer: 24

Adaptation Learning Function: Gradient descent with momentum weight and bias learning function

No. of Neurons in Input Layer: 4

Performance Function: MSE

Transfer Function: Log sigmoid transfer function

Epochs : 10000

Goal : 0.001

Learning Rate : 0.5

Epochs made : 9733

Network of Ex-17

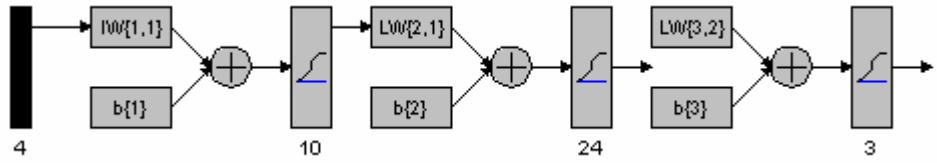

Fig 6.2 Network Architecture of Ex-17

In *Fig 13* Input layer is comprising of 4 neurons representing: 1) Voltage 2) Current 3) Travelling speed 4) Nozzle to plate distance and here we had selected the two hidden layers. In first hidden layer we had selected 10 neurons and in the second hidden layer we had selected 24 neurons .Output

layer is comprising of 3 neuron representing Bead height Bead width and Penetration.

While selecting the number of neurons in hidden layers it has to be with trial and error method as there is no hard based rule for selection of neurons so that is why several computational experiments is required to arrive at a solution and we had performed several computational experiments ,some of them has been shown here.

Training with Gradient descent with momentum back propagation

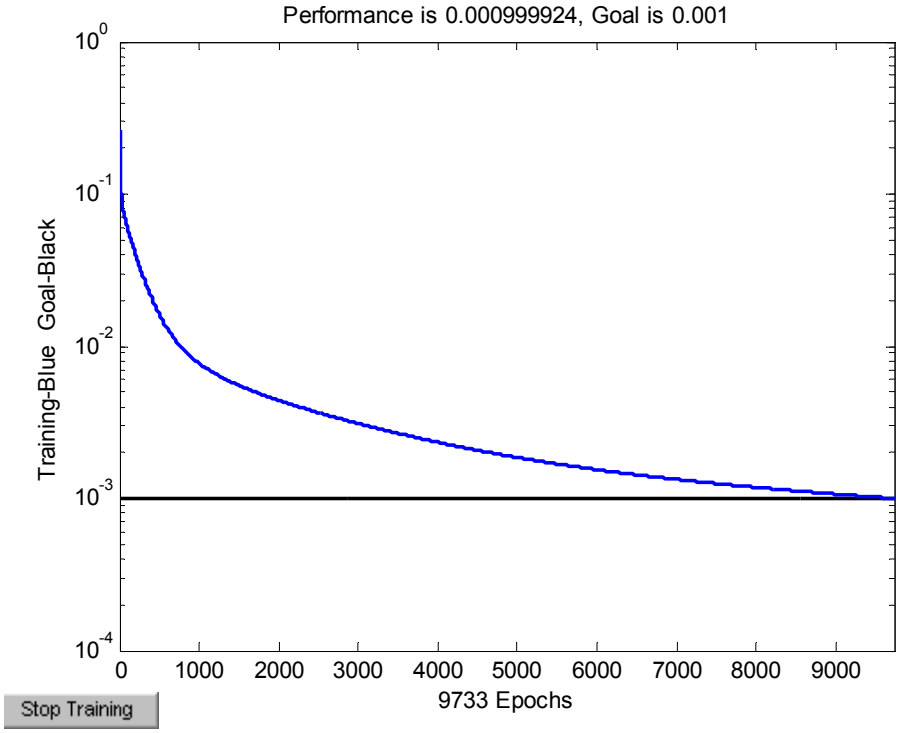

Fig 6.3 Plot Epochs v/s MSE for Ex-17.

This architecture was trained with neural network parameters i.e. Feed forward Back Propogation, we selected mean square error concept, goal was set at 0.001 and learning rate was set at 0.5. The result has been shown in the Fig 14, as this is a plot of No. of Epoch versus Mean square error. In this case it was able to converge after 9733 Epochs. After converging we will get the predicted value by the network.

6.2.2 Computational Experiment No. 2

Network Name: Ex-2.1

No. of Hidden Layers: 3

Network Type: Feed Forward Back Propogation

Training Function: Gradient descent with momentum back propagation

No. of Neurons in First Hidden Layer: 12

No. of Neurons in Second Hidden Layer: 16

Adaptation Learning Function: Gradient descent with momentum weight and bias learning function

No. of Neurons in Input Layer: 4

Performance Function: MSE

Transfer Function: Log sigmoid transfer function

Epochs : 10000

Goal : 0.001

Learning Rate : 0.5

Epochs made : 8964

Network of Ex-21.

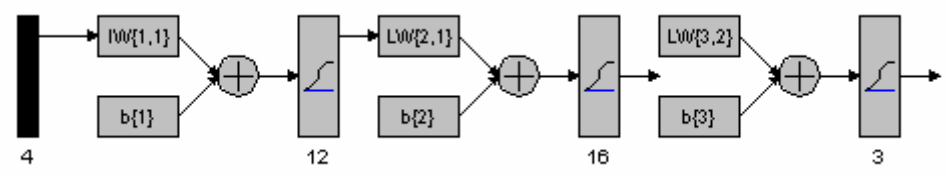

Fig 6.4 Network Architecture of Ex-21

In *Fig 13* Input layer is comprising of 4 neurons representing: 1) Voltage 2) Current 3) Travelling speed 4) Nozzle to plate distance and here we had selected the two hidden layers. In first hidden layer we had selected 12neurons and in the second hidden layer we had selected 16 neurons

.Output layer is comprising of 3 neuron representing Bead height Bead width and Penetration.While selecting the number of neurons in hidden layers it has to be with trial and error method as there is no hard based rule for selection of neurons so that is why several computational experiments is required to arrive at a solution and we had performed several computational experiments ,some of them has been shown here.

Training with Gradient descent with momentum back propagation

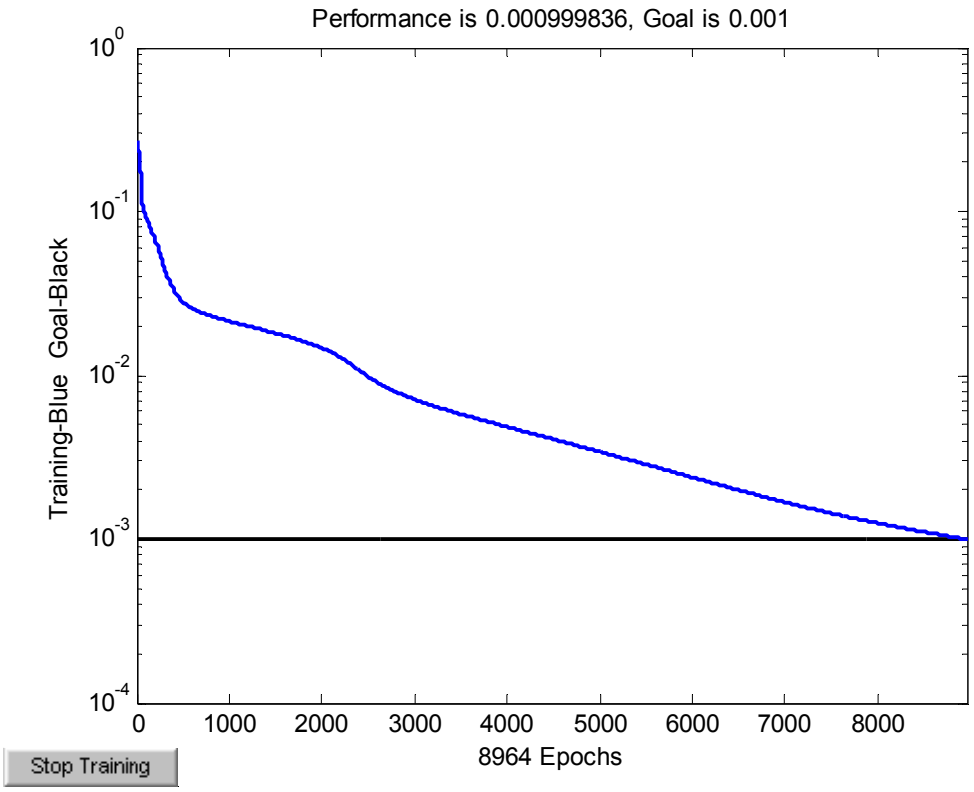

Fig 6.5 Plot Epochs v/s MSE for Ex-21.

This architecture was trained with neural network parameters i.e. Feed forward Back Propogation, we selected mean square error concept, goal was set at 0.001 and learning rate was set at 0.5. The result has been shown in the Fig 14, as this is a plot of No. of Epoch versus Mean square error. In this case it was able to converge after 8964 Epochs. After converging we will get the predicted value by the network.

6.2.3 Computational Experiment No. 3

Network Name: Ex-34.

No. of Hidden Layers: 3

Network Type: Feed Forward Back Propogation

Training Function: Gradient descent with momentum back propagation

No. of Neurons in First Hidden Layer: 10

No. of Neurons in Second Hidden Layer: 24

Adaptation Learning Function: Gradient descent with momentum weight and bias learning function

No. of Neurons in Input Layer: 4

Performance Function: MSE

Transfer Function: Log sigmoid transfer function

Epochs : 10000

Goal : 0.001

Learning Rate : 0.5

Epochs made : 5103

Network of Ex-34

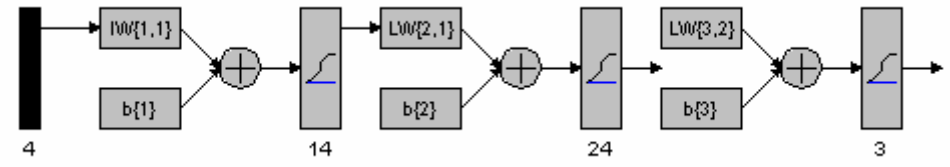

Fig 6.6 Network Architecture of Ex-34

In *Fig 13* Input layer is comprising of 4 neurons representing: 1) Voltage 2) Current 3) Travelling speed 4) Nozzle to plate distance and here we had selected the two hidden layers. In first hidden layer we had selected 10 neurons and in the second hidden layer we had selected 24 neurons .Output

layer is comprising of 3 neuron representing Bead height Bead width and Penetration.

While selecting the number of neurons in hidden layers it has to be with trial and error method as there is no hard based rule for selection of neurons so that is why several computational experiments is required to arrive at a solution and we had performed several computational experiments ,some of them has been shown here.

Training with Gradient descent with momentum back propagation

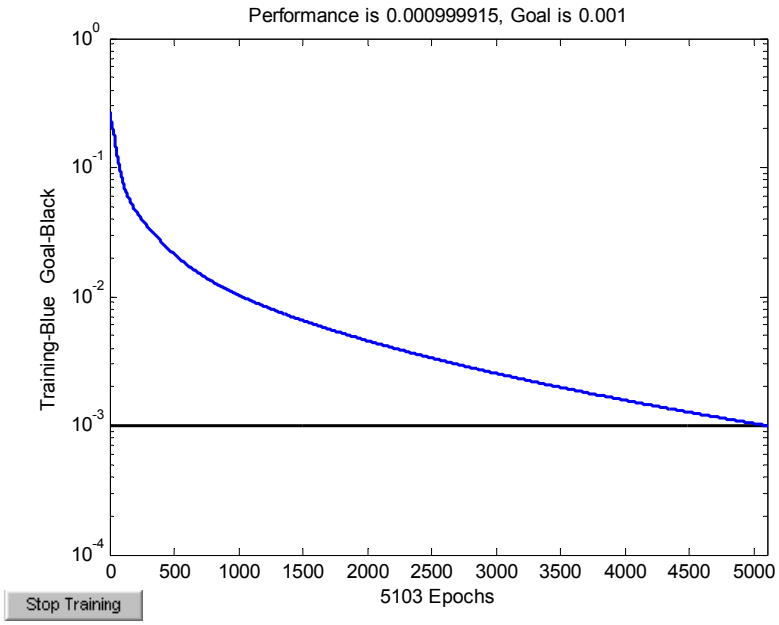

Fig 6.7 Plot Epochs v/s MSE for Ex-34.

This architecture was trained with neural network parameters i.e. Feed forward Back Propogation, we selected mean square error concept, goal was set at 0.001 and learning rate was set at 0.5. The result has been shown in the Fig 14, as this is a plot of No. of Epoch versus Mean square error. In this case it was able to converge after 5103 Epochs. After converging we will get the predicted value by the network.

The predicted values are shown in table:-2 for different set of computational experiments.

The performance of the neural network depends on the number of hidden layers, the number of neurones in the hidden layer and other learning parameters. Therefore many computational experiments were conducted with several combinations to find an optimal structure for the neural network. The performance of different ANN architectures with different learning rate which were able to converge out of various computational experiments conducted has been shown in table 6.1

Experiment No.	ANN structure	Training Function	Learning Rate	Momentum Coefficient	Epochs made
Ex-17	4-10-24-3	trainGDM	0.5	0.5	9733
Ex-21	4-12-16-3	trainGDM	0.5	0.5	8964
Ex-23	4-12-20-3	trainGDM	0.5	0.5	9466
Ex-27	4-14-12-3	trainGDM	0.5	0.5	9934
Ex-32	4-14-20-3	trainGDM	0.5	0.5	9602
Ex-33	4-14-22-3	trainGDM	0.5	0.5	7451
Ex-34	4-14-24-3	trainGDM	0.5	0.5	5103
Ex-41	4-14-12-3	trainGDA	0.5	0.5	2068
Ex-42	4-14-12-3	trainGDM	0.5	0.5	8532
Ex-45	**4-11-17-3**	**trainGDM**	**0.5**	**0.9**	**7615**
Ex-47	4-14-22-3	trainGDM	0.7	0.5	8678
Ex-49	4-16-16-3	trainGDM	0.3	0.9	9920
Ex-50	4-20-21-3	trainGDM	0.2	0.9	8766
Ex-51	4-12-15-3	trainGDM	0.3	0.9	6543
Ex-55	4-14-17-3	trainGDM	0.3	0.9	8.741

Table 6.1 Performance of different ANN architectures

The appropriate neural network structure for predicting bead geometry was chosen by trial and error method.In this work, the structure of neural network was 4-11-17-3 (11 neurons in 1st hidden layer ,17 neurons in 2nd hidden layer and 3 neurons in the output layer).The network was trained for 7615

iterations. The result of the test are summarised in table 6.2.The test data are boldface in the table and these sets of data were not used for training the network. .The scatter diagram of trained and tested dataset is shown in fig (a,b & c).Thus the network was able to predict with significant accuracy.

Weld No.	Experimental result				Neural Network result		
	H	W	P		H	W	P
1	1.5	11.1	3.2		1.8	11.2	3.1
2	1.9	14.1	5.1		1.8	13.8	4.8
3	**3.1**	**11.1**	**3.7**		**3.9**	**10.4**	**4.5**
4	2.2	13.0	7.2		2.2	12.6	7.1
5	1.2	10.7	2.4		1.0	10.5	2.9
6	3.1	10.8	2.6		2.7	10.3	2.9
7	**2.8**	**10.6**	**3.7**		**2.5**	**11.1**	**3.9**
8	1.8	11.4	5.1		1.9	11.4	4.8
9	2.8	9.5	2.4		3.0	10.0	2.8
10	1.8	12.8	3.7		1.7	12.6	3.3
11	5.7	9.5	3.2		5.8	10.1	3.6
12	**3.5**	**12.8**	**6.2**		**2.9**	**13.2**	**5.9**
13	2.2	9.0	3.2		2.3	9.1	3.6
14	2.5	10.1	3.0		2.3	9.9	2.8
15	4.8	9.2	4.0		4.7	9.2	3.9
16	2.5	9.0	5.6		2.4	9.1	5.4
17	2.8	10.6	4.0		2.7	10.6	3.6
18	**3.0**	**8.4**	**2.0**		**3.9**	**8.7**	**2.2**
19	2.2	11.1	3.4		2.4	11.5	3.4
20	1.2	10.6	3.7		1.4	10.7	2.9
21	3.8	10.7	7.6		4.1	10.5	7.1
22	2.8	10.7	3.7		2.7	10.6	3.6
23	3.1	11.7	5.0		2.9	11.9	5.0
24	1.9	11.3	3.2		1.8	11.1	3.7
25	**1.2**	**10.2**	**4.8**		**1.5**	**11.3**	**5.0**
26	4.8	10.7	3.4		4.3	9.7	3.4
27	2.6	10.8	3.4		2.7	10.6	3.6

Table 6.2 Comparision of experimental and neural network results.

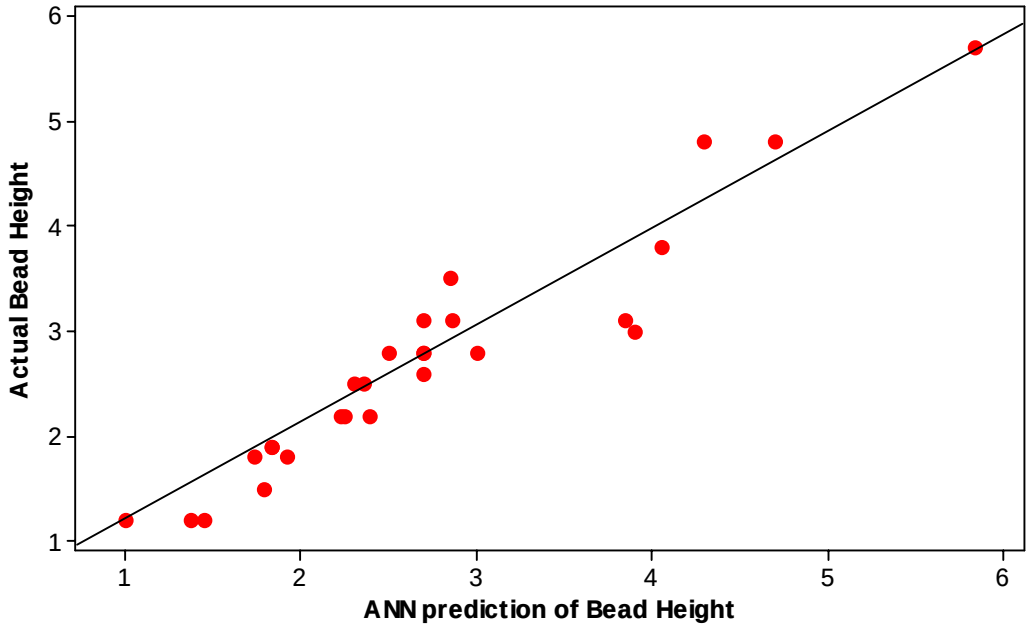

Fig 6.8 (a) Scatter Plot of ANN prediction vs. Actual Bead Height.

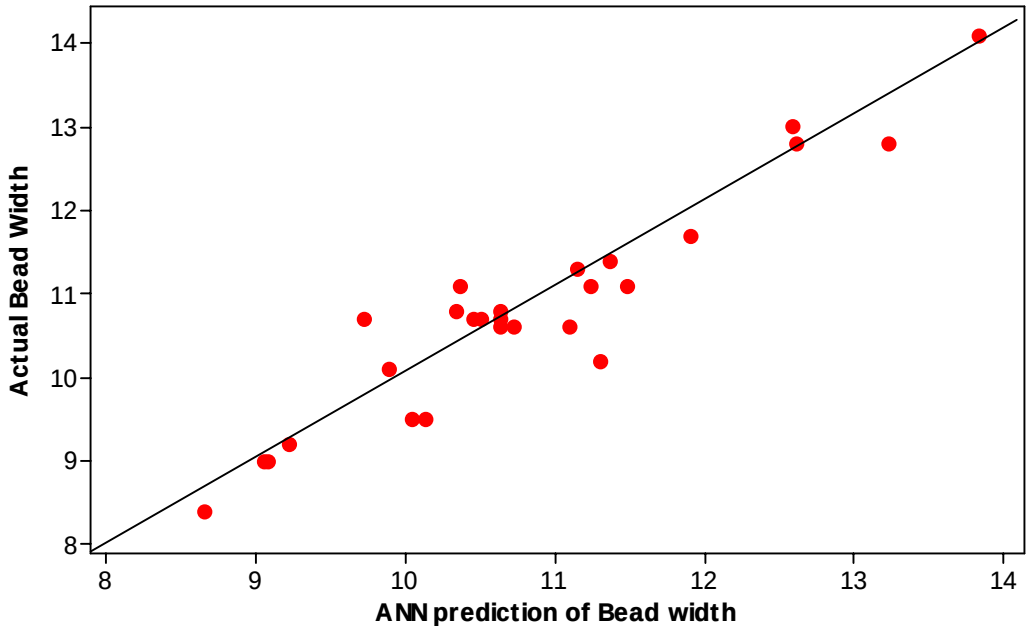

Fig 6.8 (b) Scatter Plot of ANN prediction vs. Actual Bead Width.

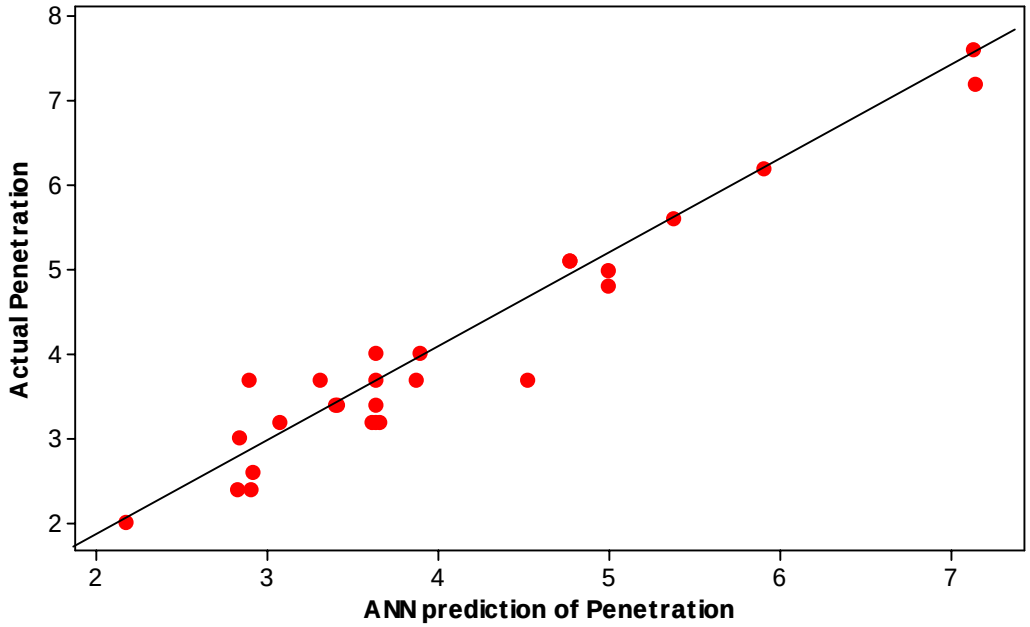

Fig 6.8 (c) Scatter Plot of ANN prediction vs. Actual Bead Penetration.

6.3 Results and Discussions:

We tried with different architecture of artificial neural network in computational experiments by changing learning rate, error goal, neurons in different layer. The network was able to converge in many of the computational experiments and when tested with test data the network was exhibiting reasonably good predictive capability.

Chapter – 7

CONCLUSION AND FUTURE SCOPE

7.0 CONCLUSION AND FUTURE SCOPE

7.1 Conclusion

The following conclusion were arrived at from the study of the effects of welding process parameters on weld bead geometry when bead-on-plate welds are deposited using SAW process.

- The Fractional Factorial technique can be employed easily for developing mathematical model for predicting weld-bead geometry within the workable region of control parameters in the SAW.
- RSM can be used effectively in analysing the cause and the effect of process parameters on response. The RSM is also used to draw contour graphs for various responses to show the interaction effects of different process parameters.
- The values of weld bead penetration, weld bead width and weld bead height decrease with the increase in welding speed.
- As the nozzle-to-plate distance increases, penetration and bead width decrease, but bead height increases.
- Back – propagation neural network used for modelling the weld bead geometry and the analysis carried out for this confirms that artificial neural networks are powerful tools for analysis and modelling .The results indicate that neural network can yield fairly accurate results.

7.2 Scope for future work

- Process parameters used in this study were arc voltage, current, welding speed and nozzle-to-plate distance. Study can be done by selecting more parameters such as multiple wire electrode, electrode wire size, flux type etc.
- RSM can be used for making analysis of HAZ and other responses of SAW process.

REFERENCES:

[1] George E. Cook, Robert J. Barnett, Kristinn Andersen, Alvin M. Straw, "Weld Modelling and Control Using Artificial Neural Networks," IEEE, (1993) 2181-2189.

[2] N.Murgan, R.S. Parmar, "Effect of Process Parameters on the geometry of the bead in the automatic surfacing of stainless steel", Journal of Materials Processing Technology.41 (1994) 381 – 398.

[3] R.S. Chandel, H.P. Seow, F.L. Cheong, "Effect of increasing deposition rate on the bead geometry of submerged arc welds" ,Journal of Materials Processing Technology.72 (1997)124 – 128.

[4] Ping Li, M.T.C. Fang, J. Lucas, "Modelling of submerged arc weld beads using self –adaptive offset neural networks", Journal of Materials Processing Technology.71(1997)288-298.

[5] V. Gunaraj, N. Murugan, "Application of response surface methodology for predicting weld bead quality in submerged arc welding of pipes ", Journal of Materials Processing Technology 88 (1999) 266-275.

[6] J.I. Lee, K.W. Um, "A prediction of welding process parameters by prediction of back-bead geometry" , Journal of Materials Processing Technology.108 (2000)106-113.

[7] G. Lothongkum, E. Viyanit, P. Bhandhubanyoung, "Study on the effects of pulsed TIG welding parameters on delta-ferrite content, shape factor and bead quality in orbital welding of AISI316L stainless steel plate", Journal of Materials Processing Technology.110 (2001)233 – 238.

[8] D.S. Nagesh, G.L. Datta, “Prediction of weld bead geometry and penetration in shielded metal-arc welding using artificial neural networks”, Journal of Materials Processing Technology.28 Jan 2002.

[9] I.S. Kim, J.S. Son, C.E. Park, C.W. Lee, Yarlagadda K.D.V. Prasad, “ A study on prediction of bead height in robotic arc welding using a neural network” Journal of Materials Processing Technology.130-131 (2002)229– 234.

[10] Ill-Soo Kim, Joon-Sik Son, Sang-Heon Lee, Prasad K.D.V. Yarlagadda, “Optimal design of neural networks for control in robotic arc welding”, Robotics and Computer-Integrated Manufacturing 20 (2004) 57–63.

[11] D. Kim, M. Kang, and S. Rhee, “Determination of Optimal Welding Conditions with a Controlled Random Search Procedure”, Welding Journal,(2005) 125-s – 130-s.

[12] N. Murugan, V. Gunuraj, “Prediction and control of weld bead geometry and shape relationships in submerged arc welding of pipes.” , Journal of Materials Processing Technology 168 (2005) 478-487

[13] Z. Sterjovski, D. Nolan. K.R. Carpenter, D.P. Dunne, J. Norrish, “Artificial neural networks for modelling the mechanical properties of steels in various applications.” ,Journal of Materials Processing Technology 170 (2005) 536-544.

[14] Z Win, R P Gakkhar, S C Jain, and M Bhattacharya, “ Parameter optimization of a diesel engine to reduce noise, fuel consumption, and exhaust emissions using response surface methodology.” , IMechE Vol.219 Part D , 2005.

[15] P Thangavel, V Selladurai, and R Shanmugam, “Application of response surface methodology for predicting flank wear in turning operation.”, IMechE Vol.220 Part B , 2006.

[16] Godfrey C. Onwubolu, Shivendra Kumar.” Response surface methodology-based approach o CNC drilling operations.”, Journal of Materials Processing Technology 171 (2006) 41-47.

[17] Veerendra Singh, Vilas Tathavadkar, S. Mohan Rao, K.S. Raju, “Predicting the performance of submerged arc furnace with varied raw material combinations using artificial neural network”, Journal of Materials Processing Technology, 183(2007) 111-116.

[18] Erdal Karadeniz , Ugur Ozsarac, Ceyhan Yildiz, “The effect of process parameters on penetration in gas metal arc welding processes” Materials and Design 28 (2007) 649–656.

[19] Parikshit Dutta, Dilip Kumar Pratihar, “Modeling of TIG welding process using conventional regression analysis and neural network based approaches” , Journal of Materials Processing Technology 184 (2007) 56-68.

[20] M B Parappagoudar, D K Pratihar, G L Datta, “ Non-linear modelling using central composite design to predict green sand mould properties”, IMechE Vol.221 Part B , 2007.

[21] P B Bacchewar, S K Singhal, and P M Pandey, “ Statistical modelling and optimization of surface roughness in selective laser sintering process”, IMechE Vol.221 Part B , 2007.

[22] A.M.K. Hafiz, A.K.M.N. Amin, A.N.M. Karim, M.A. Lajis, " Development of surface roughness prediction model using response surface methodology in high speed end milling of AISI H13 tool steel.", IEEE, 2007.

[23] Serdar Karaoglu, Abdullah Secgin , "Sensitivity analysis of submerged arc welding process parameters", Journal of Materials Processing Technology.202 (2008)500-507.

[24] Abdulkadir Cevik, ,M. Akif Kutuk,Ahmet Erklig,Ibrahim H. Guzelbey, "Neural network modeling of arc spot welding", Journal of Materials Processing Technology 202 (2008) 137– 144.

[25] K. Manikya Kanti, P. Srinivasa Rao, "Prediction of bead geometry in pulsed GMA welding using back propagation neural network", journal of materials processing technology 200 (2008) 300–305.

[26] Keshav Prasad & D. K. Dwivedi,"Some investigations on microstructure and mechanical properties of submerged arc welded HSLA steel joints", Journal of Advance Manufacturing Technology (2008) 36:475–483.

[27] Kishor P. Kolhe, C.K. Datta, "Prediction of microstructure and mechanical properties of multipass SAW", Journal of Materials Processing Technology 197 (2008) 241-249.

[28] Sukhomay Pal, Surjya K. Pal, Arun K. Samantaray, " Artificial neural network modeling of weld joint strength prediction of a pulsed metal inert gas welding process using arc signals", Journal of Material Processing Technology 202 (2008) 464-474.

[29] N. Aslan, “Application of response surface methodology and central composite rotatable design for modelling and optimization of a multi-gravity separator for chromite concentration.” , Power Technology 185 (2008) 80-86.

[30] Bappa Acherjee, Dipten Misra, Dipankar Bose, K. Venkadeshwaran, “Prediction of weld strength and seam width for laser transmission welding of thermoplastic using response surface methodology”, Optics and Laser Technology 41(2009) 956-967.

[31] V Balasubramanian, A K Lakshminarayanan, R Varahamoorthy, S Babu, “ Application of response surface methodology to prediction of dilution in plasma transferred arc hardfacing of stainless steel on carbon steel.”, Journal of Iron and Steel Research, International, 2009, 16(1), 44-53.

[32] http://www.welding-technology-machines.info/physics-of-welding/weld-bead-geometry.htm.

[33] http://en.wikipedia.org/wiki/Artificial_neural_network**.**

[34] http://www.doc.ic.ac.uk/~nd/surprise_96/journal/vol4/cs11/report.html# Introduction to neural networks

[35] Neural Network by Christos Stergiou and Dimitrios Siganos

[36] Stefano Nolfi Domenico Parisi, Evolution of Artificial Neural Networks, I nstitute of Psychology, National Research Council, Rome.

[37] A.C. Davies, Welding Science and technology,Vol-1,Ninth Edition Cambridge university press.

[38] R.S. Parmar, Welding Process and Technology, Second edition, Khanna Publication.

[39] Rudra pratap, Getting started with Matlab7,Indian edition ,Oxford university press.

[40] Douglas C. Montgomery, Design and Analysis of Experiments.5th edition, John Wiley & Sons (Asia).

[41] D.N. Elhance, Veena Elhance, B.M. Agarwal, Fundamental of Statistics,Liind Rep. Edition, Kitab Mahal Publications.

[42] Raymond H. Myers, Douglas C. Montgomery, Response Surface Methodology Process and Product Optimization using Designed Experiments, Second Edition, John Wiley & Sons, INC.

[43] Ronald E. Walpole, Raymond H. Myers, Sharon L. Myers, Keying ye, Probability & Statistics for Engineers & Scientists, Seventh Edition, Dorling Kindersley (India) Pvt. Ltd.